

Issue 2  
Volume 1  
June, 2024

ISSN 2818-0313  
DOI Prefix : 10.62252

# *Naturalis*



# *Scientias*

[www.naturalisscientias.com](http://www.naturalisscientias.com)



## TABLE OF CONTENTS

### *ORIGINAL ARTICLES*

Analysis of the data in Jingwen Mao's paper on the stable isotopes ( $\delta D_{H_2O}$ , $\delta^{18}O_{H_2O}$ , and $\delta^{34}S$ ) of the gold deposits in Jiaodong Peninsula, China.....	137
Indium use, resource, market and ore deposit type .....	152
Temporal and spatial distribution and genesis of primary indium deposits around the world .....	167
Joy and Sorrow; Sorrow and Joy .....	181
My impressions after reading the book Less Words but Earnestly Practice-- My Father Chuangan Zhang .....	186



## Original Article

**Analysis of the data in Jingwen Mao's paper on the stable isotopes ( $\delta D_{H_2O}$ ,  $\delta^{18}O_{H_2O}$ ,  $\delta^{34}S$ ) of the gold deposits in Jiaodong Peninsula, China**Fa Han<sup>1</sup> **Abstract**

In 2008, Jingwen Mao published a paper on the stable isotopes of gold deposits in the Jiaodong Peninsula. The paper has a series of problems in obtaining  $\delta D_{H_2O}$  and  $\delta^{18}O_{H_2O}$  of ore-forming fluids and interpreting  $\delta^{34}S$  data. ① In order to obtain  $\delta D_{H_2O}$  and  $\delta^{18}O_{H_2O}$  data of ore-forming fluids, Jingwen Mao selected sericite (a total of 25 samples) as the target mineral. Sericite is not an independent mineral and has no fixed molecular formula. New research has shown that it is a fine-grained aggregate composed of muscovite, illite, and sodium mica (at least muscovite and sodium mica). The water content in sericite is very complicated, including structural water, interlayer water, fissure water, primary and secondary inclusion water. Jingwen Mao extracted water from sericite by crushing, and this mixed water cannot represent the ore-forming fluids. It is unreliable to determine the source of ore-forming fluids using  $\delta D_{H_2O}$  measured by this kind of mixed water. ② So far, no oxygen isotope fractionation coefficient relationship between sericite and water has been obtained, whether through theoretical calculation or experimental research. In order to calculate the  $\delta^{18}O_{H_2O}$  of ore-forming fluids by measuring the  $\delta^{18}O$  of sericite, Jingwen Mao used the oxygen isotope fractionation coefficient relationship between muscovite and water for calculation, which is completely wrong. ③ The data of  $\delta^{18}O_{H_2O}$  and  $\delta D_{H_2O}$  of ore-forming fluids obtained by Jingwen Mao using sericite are very different from the relevant data obtained by previous researchers using quartz as the target mineral (131 samples). Based on those unreliable data, Jingwen Mao believed that the ore-forming fluids came from the mixed source of crust and mantle, while the relevant data of previous researchers proved that the ore-forming fluids came from the products of atmospheric precipitation exchanging with Jiaodong Group metamorphic rocks under different temperatures and different W/R ratios. ④ For the relationship between the high or low  $\delta^{34}S$  value of sulfide minerals and the large or small  $\log fO_2$  value, Jingwen Mao's explanation is completely opposite to the research results of Ohmoto and Wang. Ohmoto believed that the two were negatively correlated, while Jingwen Mao believed that they were positively correlated. This is a common sense mistake.

**Key words:** problem; the stable isotopes  $\delta D_{H_2O}$ ,  $\delta^{18}O_{H_2O}$  &  $\delta^{34}S$ ; source of ore-forming fluid; sericite; genesis; Jiaodong gold deposits

---

**Affiliation Info:** <sup>1</sup> Institute of Mineral Deposits, Chinese Academy of Geological Sciences, Beijing, 100037, China

**Article Info:** Received: 30 May 2024 / Revised: 12 June 2024 / Accepted: 26 June 2024 / Published Online: 30 June 2024.  
www.naturalisscientias.com

**Authors' Contact Info:** Han, F: hfandxrl@126.com

**Citation:** Han, F. 2024. Analysis of the data in Jingwen Mao's paper on the stable isotopes ( $\delta D_{H_2O}$ ,  $\delta^{18}O_{H_2O}$ ,  $\delta^{34}S$ ) of the gold deposits in Jiaodong Peninsula, China. *Naturalis Scientias*, 1 (2): 137-151. DOI: <https://doi.org/10.62252/NSS.2024.1010>.

**Copyright** © 2024 by the author. Published by *Naturalis Scientias*. This is an open access article under the Creative Commons Attribution-NonCommercial 4.0 International (CC BY-NC 4.0) License. (<https://creativecommons.org/licenses/by-nc/4.0/>).

**Corresponding Author** : Han, F; Research Professor; Email: hfandxrl@126.com

## 1 Introduction

The Jiaodong Peninsula gold deposit in China is a world-class super-large gold deposit. A lot of research has been done on the geology of the deposit, the source of ore-forming fluids and the genesis of the deposit. The research results of this deposit are of great significance to the genesis of gold deposits and the guidance of gold prospecting. In the paper titled “the relationship of mantle-derived fluids to gold metallogenesis in the Jiaodong Peninsula: Evidence from D–O–C–S isotope systematics” (hereinafter referred to as the 2008 paper) published in 2008 by Jingwen Mao<sup>1</sup>, there are a series of problems in the determination of hydrogen and oxygen isotopes and the interpretation of sulfur isotope data of gold deposits in the region, which are described as follows.

## 2 Selection of target mineral samples

The best target mineral for studying the hydrogen and oxygen isotope composition of ore-forming fluids in hydrothermal endogenous metal deposits is quartz. The reasons are as follows:

- Quartz is widely distributed and is commonly found in metamorphic rocks, intermediate-acidic intrusive rocks, and various endogenous metal deposits.
- Quartz is stable, hard, and has no cleavage, and its primary fluid inclusions are easy to preserve.
- Quartz has good transparency, and its primary fluid inclusions are simple and reliable for temperature measurement.
- Quartz has a single chemical composition ( $\text{SiO}_2$ ) and does not contain structural water. So, it is very reliable to use its primary fluid inclusion water to measure  $\delta\text{D}_{\text{H}_2\text{O}}$ .

Although the oxygen in the water of the quartz’s primary fluid inclusions will undergo isotopic exchange with the oxygen in the quartz lattice, the ratio of the two is very different, so the effect on the quartz  $\delta^{18}\text{O}$  composition can be ignored.

The oxygen isotope fractionation coefficient of the quartz-water system and its difference in fractionation coefficients in different temperature ranges have the highest degree of research and are the most accurate.

Therefore, it has become a consensus in the academic community to use the oxygen isotope fractionation equation of the quartz-water system to calculate the  $\delta^{18}\text{O}_{\text{H}_2\text{O}}$  of ore-forming fluids.

In fact, it is common sense for ore deposit geologists to use quartz as a target mineral to determine the source of ore-forming fluids. For example, the earliest study on determining the source of ore-forming fluids in volcanic massive sulfide deposits was completed by Japanese scholars using quartz in black ore deposits. The results showed that the ore-forming fluid of this type of deposit is a mixture of seawater and magmatic water<sup>2</sup>.

## 3 Analysis and problem

In his 2008 paper, Jingwen Mao measured hydrogen and oxygen isotopes on 37 single mineral samples from 9 deposits in the study area. Unlike other researchers, Mao measured 7 samples of potassium feldspar and 25 samples of sericite for the altered broken rock type and quartz vein type deposits (Tables 1 and 2), but he did not use quartz as the target mineral.

During the analytical process, the method of obtaining elemental hydrogen is as follows: first, the water in the fluid inclusions in the mineral is extracted by crushing, and then the water reacts with zinc to produce hydrogen<sup>1</sup>.

There are the following problems here:

**Table 1.** Comparison of  $\delta^{18}\text{O}_{\text{H}_2\text{O}}$  (‰) of ore-forming fluids and  $\delta\text{D}_{\text{H}_2\text{O}}$  (‰) of water in quartz inclusions in different gold deposits of Jiaojia type at different mineralization stages with the corresponding data of sericite and potassium feldspar

Mine	Metallogenic stage	Mineralization type	Analyzed mineral	$\delta^{18}\text{O}$	$\delta^{18}\text{O}_{\text{H}_2\text{O}}$ ①	$\delta\text{D}_{\text{H}_2\text{O}}$	Source
Taishang	I	Massive quartz vein	quartz	12.1(2)	4.7	-78(1)	[11]
Hobu			quartz	11.9 (2)	4.5		
Cangshang			quartz	12.7 (3)	5.3	-77 (1)	
Sanshandao			quartz	14.2 (2)	6.9	-62 (2)	
Dayigezhuang			quartz	10.9 (1)	3.5	-78 (1)	
			average	12.4±1.2	4.7±1.2	-73±7.8	
Taishang	II	Sulfide quartz vein	quartz	12.2 (4)	2.8	-85 (2)	[11]
Jiaojia			quartz	11.4 (2)	2		
Hobu			quartz	13.1 (1)	3.7		
Cangshang			quartz	14.1 (1)	4.7	-82 (1)	
Sanshandao			quartz	14.7 (2)	5.3	-71 (1)	
Dayigezhuang			quartz	11.3 (4)	1.9	-78 (2)	
Xincheng			quartz	13.9 (4)	4.5	-87 (3)	
			average	13.2±1.3	3.5±1.3	-80±6.3	
Taishang	III	Quartz-calcite vein	quartz	15.4 (3)	4.5	-91 (1)	[11]
Xincheng			quartz	15.0 (2)	4.1		[12]
Sanshandao			quartz	13.4 (2)	2.5	-92 (1)	[11]
Jiaojia			quartz	13.7 (1)	2.8	-107 (1)	
			average	14.4±1.0	3.5±1.0	-92±0.6	
Sanshandao	II ②③	Quartz sulfide vein	Sericite	11.7 (6)	7.85	-53.6 (6)	[1]
Cangshang			Sericite	11.12 (5)	7.97	-51.8 (5)	
Jiaojia			Sericite	9.9 (3)	6.75	-60.0 (3)	
Wangershan			Sericite	9.58 (4)	6.44	-57.3 (4)	
Dayigezhuang ②			Sericite	9.22 (5)	6.01	-58.4 (5)	
			average	10.3±0.95	7.0±0.78	-56.2±3	
Jiaojia	II ②③	Quartz sulfide vein	K-spar	10.1 (2)	4.27	85.5±0.5 (2)	[1]
Dayigezhuang ②			K-spar	8.87 (3)	3.03	-78±11.3 (3)	
			average	9.5 ±0.62	3.65±0.62	-81.8±3.8	

Note: ① According to the best estimate of homogenization temperature: 300°C in the first mineralization stage, 250°C in the second mineralization stage, and 220°C in the third mineralization stage. ② Jingwen Mao classified the Dayigezhuang gold deposit as a quartz vein-type gold deposit, but Li<sup>10</sup> and Zhang<sup>11</sup> believed that the deposit belonged to the altered broken rock type (Jiaojia type) gold deposit. ③ When Jingwen Mao used sericite and potassium feldspar to determine the hydrogen and oxygen isotope composition of the ore-forming fluid, he did not divide the mineralization stage. According to the inference of its mineralization type, the target minerals he selected may belong to the mineralization stage II. ( ) is the number of samples

Jingwen Mao did not conduct a microscopic study on potassium feldspar or sericite, and did not describe the size of its mineral grains, the relationship of paragenesis, the freshness of the minerals, and the state of preservation (i.e., whether there are microscopic cracks).

There is no description of whether there are fluid inclusions in the minerals, whether there are secondary inclusions, and their number and size. In particular, the grain size of sericite is generally very small, and the cleavage is well developed, so it is doubtful whether there are primary fluid inclusions in it.

**Table 2.** Comparison of  $\delta^{18}\text{O}_{\text{H}_2\text{O}}$  (‰) of ore-forming fluids and  $\delta\text{D}_{\text{H}_2\text{O}}$  (‰) of water in quartz inclusions, sericite and feldspar at different mineralization stages in different Linglong-type (quartz vein-type) gold deposits

Mine	Metallogenic stage	Mineralization type	Minerals	$\delta^{18}\text{O}$	$\delta^{18}\text{O}_{\text{H}_2\text{O}}$	$\delta\text{D}_{\text{H}_2\text{O}}$	Source
Qixia	I	Beresitization	Quartz (4)	12.7±0.66	3.78±0.67	-62.5±7.8	[14]
Lingllon		Pyrite-quartz vein	Quartz (2)		3.25±1.79	-62.7±4.8	[13]
Rushan		Pyrite-quartz vein	Quartz (4)	10.9±1.45	2.06±1.51		[9] <sup>①</sup>
Qixia		Pyrite-quartz vein	Quartz (1)	12.53	5.3	-66.4	[8]
Denggezhuang		Pyrite-quartz vein	Quartz (2)	14.1±0.52	5.29±1.17	-78.9±4.4	[10]
			average		12.6±1.13	3.94±1.24	-67.6±6.6
Qixia	II	Pyrite-quartz vein	Quartz (5)	12.24±0.8	1.16±0.89	-78.2±9.3	[14]
Qixiaq		Sulfide-quartz vein	Quartz (1)	12.56	2.67	58.5	[8]
Denggezhuang		Au-bearing quartz vein	Quartz (3)	13.53±1.9	4.57±1.97	-77±5.7	[10]
Tangjiagou		Sulfide-quartz vein	Quartz (2)	10.47±1.7	3.05±0.82	-72±1.5	
			average		12.20±1.1	2.86±1.21	-71.4±7.8
Qixia	III	Quartz-carbonate vein	Quartz (4)	12.25±1.1	-2.4±1.03	-91.3±2.6	[14]
Rushan		Siderite-quartz vein	Quartz (1)	11.6	0.06		[9]
Lingnan		Au-bearing pyrite	Quartz (3)		-4.7±0.1	-86±0.8	[16]
Jiuqu		Pyrite-quartz vein	Quartz (2)		-8.4±1.8	-100±10.0	
Shilipu		Carbonate-quartz vein	Quartz (21)	9.7	-3.6 (15)	-84 (7)	[17]
			average		11.18±1.1	-4.77±2.3	-90.3±6.2
Denggezhuang	II	Sulfide-quartz vein	Sericite (2)	9.6±0.9	6.45±0.9	-66.5±9.5	[1]
Denggezhuang	II	Sulfide-quartz vein	K-spar (2)	8.85±0.3	3.02±0.25	-86±1.0	

Note: ① The  $\delta^{18}\text{O}_{\text{H}_2\text{O}}$  here is calculated by the original author Li<sup>9</sup> based on the ore-forming temperature of 295°C, while Li<sup>13</sup> calculated it based on the ore-forming temperature of 265°C. This paper uses the latter. The number of samples is in parentheses

When the above crushing method is used to extract water from fluid inclusions in minerals, water in secondary inclusions, cleavage cracks, and microscopic cracks is also extracted at the same time. In addition, there is interlayer water in sericite, which obviously cannot represent the water of the ore-forming fluid.

Sericite also contains structural water, and it is inevitable that the hydrogen in its structural water will undergo isotope exchange with the hydrogen in the inclusion water. Therefore, its  $\delta D_{H_2O}$  result is unreliable.

Regarding the oxygen isotope problem, there is no experimental research result on the oxygen isotope fractionation coefficient of the sericite-water system. Jingwen Mao used the oxygen isotope fractionation coefficient of the muscovite-water system instead to calculate the oxygen isotope comparison of the fluid water in equilibrium with sericite.

Is this feasible?

To answer this, it is necessary to explain what sericite is. The old traditional view is that sericite is a fine-grained aggregate (variant) of muscovite. It is not an independent mineral and has no fixed molecular formula. Therefore, Wang (1965) believed that compared with muscovite, sericite may contain slightly less potassium and slightly more water<sup>3</sup>. However, new research in the Western mineralogy community believes that very fine-grained and irregular aggregates of white mica minerals are named sericite, and white mica minerals are typically composed of muscovite, illite and sodium mica<sup>4</sup>. Of course, it is not ruled out that in a few cases, sericite is just a fine-grained variant of muscovite or sodium mica<sup>5</sup>. Dietrich believes that a variant composed of fine transparent crystals of muscovite or sodium mica (or both) is usually called sericite<sup>6</sup>. This variant of fine transparent crystals has a silky luster.

Because of this, sericite is not included in the theoretically calculated oxygen isotope fractionation coefficients of the 72 minerals and water so far. Sericite is also not included in the experimentally measured oxygen isotope fractionation coefficients of the 46 minerals and water<sup>7</sup>.

Obviously, it is wrong for Jingwen Mao to use the oxygen isotope fractionation coefficient of the muscovite-water system to replace the oxygen isotope fractionation coefficient of the sericite-water system. There are uncertainties in the interpretation of the  $\delta^{18}O_{H_2O}$  values of his 25 sericite single minerals.

As for the Jiaodong gold deposits, preliminary research found that 14 predecessors<sup>8-17</sup> used quartz as the target mineral to study the hydrogen and oxygen isotopes of the deposits, and measured as many as 131 samples. As far as we know, only Wang had one sample and Li had five samples that used sericite as the target mineral<sup>8-9</sup>. But, both of them did not explain how they determined the  $\delta D_{sericite}$ .

In particular, it is wrong that Li used  $1000\ln\alpha_{muscovite-water} = -22.1 \times 10^6/T^2 + 19.1$  to replace the hydrogen isotope fractionation coefficient of the sericite-water system for calculating the hydrogen isotope comparison of the ore-forming fluid. But what is worse, Li openly wrote the above hydrogen isotope fractionation relationship as  $\delta D_{sericite} - \delta D_{water} = -22.1 \times 10^6/T^2 + 19.1$  in his article<sup>9</sup>. These blatantly fake data are of course not usable. For this reason, Li (1993) did not cite the  $\delta D_{H_2O}$  and  $\delta^{18}O_{H_2O}$  data obtained by a few researchers using sericite in his monograph on the Jiaodong gold mine<sup>10</sup>. On this basis, the relevant test results are listed in Tables 1 and 2 according to the two mineralization types; namely, the Jiaojia type and Linglong type.

It must be pointed out that the test results in Tables 1 and 2 are classified and arranged according to the mineralization stages. Those test results that cannot determine the mineralization stage are not included in the tables.

#### 4 Discussion

The data and corresponding figures of hydrogen and oxygen isotopes by previous researchers using quartz as the target minerals and by Jingwen Mao using sericite and potassium feldspar as the target minerals are listed in Table 1, in the hope that through comparison, it will be clear which is right and which is wrong.

Figure 1 below is a diagram of  $\delta D_{H_2O} - \delta^{18}O_{H_2O}$  of the altered broken rock type and quartz vein type gold deposits in Jiaodong. As can be seen from Figure 1, the projection points of potassium feldspar and sericite are obviously located in two intervals. The projection point of potassium feldspar is located in the C and D evolution curve range of the water/rock exchange process, while the projection points of sericite, with a few exceptions, are all located in the range of magmatic water or metamorphic water. Why is there such a big difference between the two? This will be discussed later.

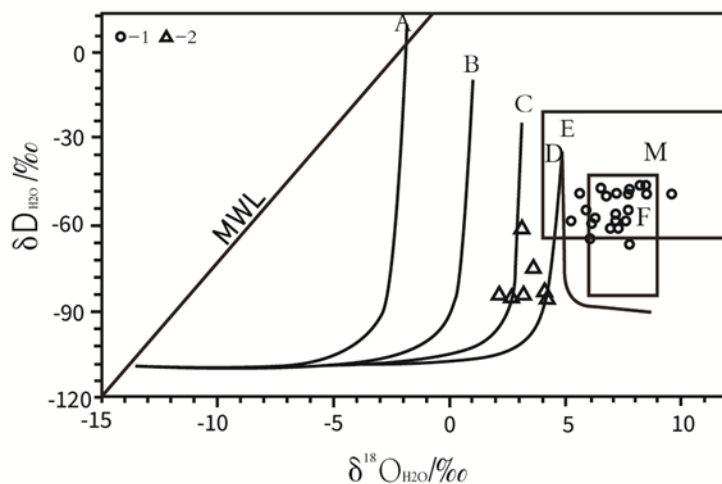


**Figure 1.**  $\delta D_{H_2O} - \delta^{18}O_{H_2O}$  diagram of altered broken rock type and quartz vein type gold deposits in Jiaodong (data quoted from Mao in the reference 1 of this paper)

1 – Sericite, 2 - Potassium feldspar

The curves A, B, C, and D in the figure are the evolution curves of atmospheric precipitation at 150°C, 200°C, 250°C and 300°C in the process of water/rock exchange, and E is the evolution curve of magmatic water at 300°C<sup>14</sup>; MWL is the atmospheric precipitation line; F and M are the isotopic compositions of magmatic water and metamorphic water.

Figure 2 is a graph showing the  $\delta D_{H_2O} - \delta^{18}O_{H_2O}$  variation of fluids in different mineralization stages of Jiaojia-type gold deposits in Jiaodong<sup>11</sup>. Zhang pointed out that the mineralization of Jiaojia-type large-scale gold deposits includes vein quartz in three different stages (but mainly in the second stage). As can be seen from Figure 2, the deposition temperature of Jiaojia-type large-scale gold deposits is between 300 °C and 200 °C, the  $\delta^{18}O_{H_2O}$  value of the fluid is around +4‰, and the  $\delta D_{H_2O}$  value changes from -70‰ to -90‰ from stage I to stage III. Combining the H and O isotopic compositions of Mesozoic atmospheric precipitation, the isotopic compositions of ore-forming hydrothermal water and temperature data, it is inferred that the ore-forming fluids of the Jiaojia-type gold deposits were formed by the exchange of Mesozoic atmospheric precipitation with intermediate-basic rocks at depths below 5 km at 350 – 400 °C, with an effective W/R ratio ranging from 0.01 to 0.05, and were cooled and deposited at around 350 °C in a buffered open system<sup>11</sup>.

Figure 3 is a diagram of the hydrogen and oxygen isotope evolution of hydrothermal fluids formed during the exchange of meteoric precipitation and magmatic water with the metamorphic rocks of the Jiaodong Group<sup>14</sup>.

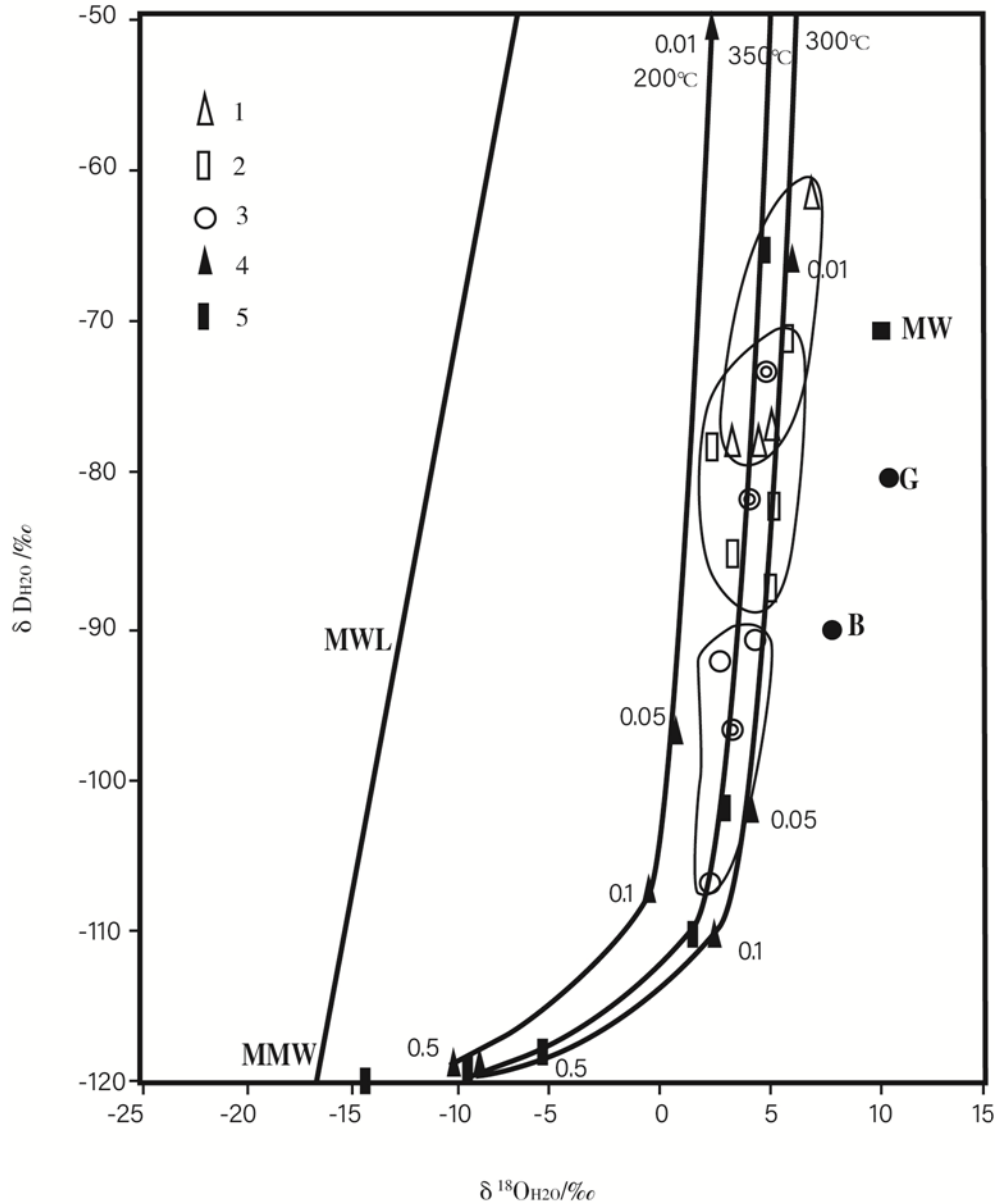


**Figure 2.**  $\delta D_{H_2O} - \delta^{18}O_{H_2O}$  variation diagram of fluids in different mineralization stages of Jiaojia-type gold deposits in Jiaodong<sup>11</sup>

Note: Initial conditions of evolution line: MW is magmatic water ( $\delta^{18}O_{H_2O} = 9.1\%$ ,  $\delta D_{H_2O} = -71\%$ ); MMW is Mesozoic atmospheric precipitation ( $\delta^{18}O_{H_2O} = -16\%$ ,  $\delta D_{H_2O} = -120\%$ ); G is granite ( $\delta^{18}O_{H_2O} = 11\%$ ,  $\delta D_{H_2O} = -80\%$ ); B is basic rock ( $\delta^{18}O_{H_2O} = 7.5\%$ ,  $\delta D_{H_2O} = -90\%$ ). 1-stage I ore-forming fluid; 2-stage II ore-forming fluid; 3-stage III ore-forming fluid; 4-The Mesozoic precipitation evolution curve of atmospheric precipitation (MMW) and granite (G) at 200 °C and 300 °C and under different W/R ratios; 5-The Mesozoic precipitation evolution curve of atmospheric precipitation (MMW) and basic rock (B) at 350 °C and under different W/R ratios

As can be seen from Figure 3, the hydrogen and oxygen isotope values of the ore-forming solutions of the Qixia gold deposit at different mineralization stages are generally different from the magmatic water evolution curve at the projection points in Figure 3, but are consistent with the meteoric precipitation evolution curve of the corresponding temperature.

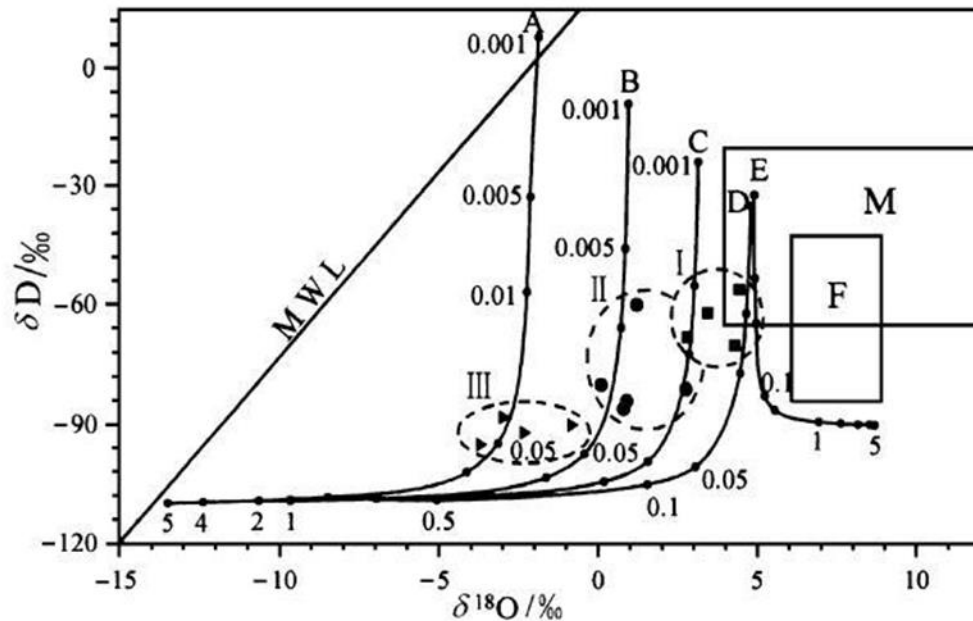


**Figure 3.** Hydrogen and oxygen isotope evolution during the exchange between atmospheric precipitation, magmatic water and metamorphic rocks<sup>14</sup>

Note: The curves A, B, C, and D in the figure are the evolution curves of atmospheric precipitation at 150 °C, 200 °C, 250 °C and 300 °C during the water/rock exchange process, and E is the evolution curve of magmatic water at 300 °C; the number corresponding to each black dot on all curves represents the effective (W/R) mass value; MWL is the atmospheric precipitation line; F and M are the isotopic compositions of magmatic water and metamorphic water; I, II, and III are the projection points of hydrothermal fluids in the early, main, and late stages of the Qixia gold deposit, respectively. The  $\delta^{18}\text{O}_{\text{H}_2\text{O}}$  values of the Jiaodong Group metamorphic rocks, magmatic water and atmospheric precipitation are 9.5‰, 9.0‰ and -15.0‰, respectively; and the  $\delta\text{D}_{\text{H}_2\text{O}}$  values are -90‰, -90‰ and -110‰, respectively. The initial parameters used to calculate the evolution curve refer to the specific situation of the Qixia gold mine. The bottom layers of metamorphic rocks in the Jiaodong area mainly include the Jiaodong Group, Jingshan Group, Fenzishan Group, and Penglai Group, etc. Among them, the Jiaodong Group is the main component of the old metamorphic basement, and the lithology belongs to the Archean greenstone belt.

For example, the projection point in the early stage of mineralization is located near the 250 – 300 °C meteoric precipitation evolution curve C and D, the projection point in the main mineralization period is located between the 200 – 250 °C curves B and C, the projection point in the late stage of mineralization is located near the 150 – 200 °C curves A and B. Although the projection point in the early stage of mineralization seems to be close to the magmatic water evolution curve E, the temperature of the hydrothermal fluid in the early stage of mineralization is not that high. From the early to the late stage of mineralization, the effective W/R ratio of the interaction between meteoric precipitation and metamorphic rocks tends to increase. The W/R ratio in the early stage of mineralization is about 0.005 - 0.01, the W/R ratio in the main mineralization period is about 0.01 - 0.05, and the W/R ratio in the late stage of mineralization is close to 0.05.

That is, the distribution of hydrogen and oxygen isotope values of the ore-forming hydrothermal fluid of the Qixia gold deposit well reflects the characteristics of meteoric precipitation after exchange with the metamorphic rocks of the Jiaodong Group under different temperatures and different W/R ratios.

As can be seen from Figure 4 below, the hydrogen and oxygen isotopes of different mineralization stages (from early to late) of the quartz vein type (the Linglong type) gold deposit gradually drift towards the rainwater line from stage I to stage IV. This indicates that as the mineralization progresses, the proportion of atmospheric precipitation in the mineralizing fluid becomes larger and larger.

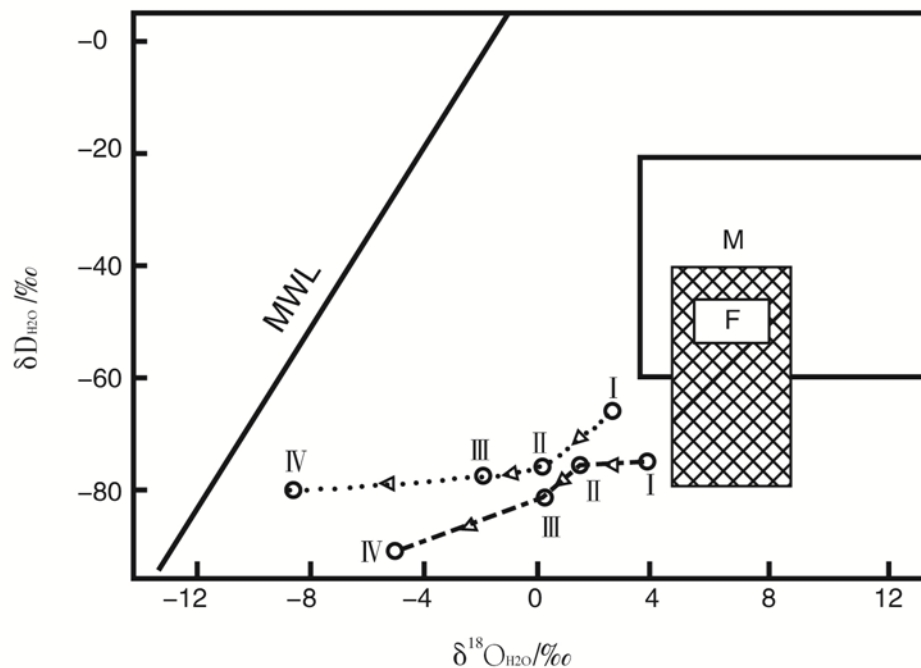


**Figure 4.**  $\delta D_{H_2O} - \delta^{18}O_{H_2O}$  relationship of ore-forming fluids in each mineralization stage of Linglong Gold Mine<sup>16</sup>

Note: I - pyrite-quartz stage; II - gold-polymetallic sulfide-quartz stage; III - gold-silver-polymetallic sulfide stage; IV - pyrite-quartz-carbonate stage. MWL is the atmospheric precipitation line, F and M are the isotopic compositions of magmatic water and metamorphic water respectively. The dotted line is the fluid inclusion in quartz, and the dashed line is the fluid inclusion in pyrite

As can be seen from Figures 2 to 4 above, whether it is the Jiaojia-type gold deposit, or the Qixia type gold deposit or the Linglong type gold deposit, the  $\delta D_{H_2O}$  and  $\delta^{18}O_{H_2O}$  values of the ore-forming fluid measured by quartz as the target mineral are generally quite different from the magmatic water area and the magmatic water evolution curve, but are consistent with the atmospheric precipitation evolution curve at the corresponding temperature. In addition, the hydrogen and oxygen isotope values of these deposits in different mineralization stages (from early to late) gradually drift toward the atmospheric precipitation line, indicating that with the progress of mineralization, the proportion of atmospheric precipitation in the ore-forming fluid is increasing. In short, these actual data well prove that the ore-forming fluid comes from the product of atmospheric precipitation exchanging with the metamorphic rocks of the Jiaodong Group under different temperatures and different W/R ratios. As Zhang pointed out, the ore-forming fluid is formed by the exchange of Mesozoic atmospheric precipitation with deep basic rocks at about 350 °C and W/R = 0.01, and then cooling in a buffered open system<sup>11</sup>. Of course, it is not ruled out that a small amount of magmatic hydrothermal fluid may be mixed in the early stage of mineralization. However, the metamorphic old basement in Jiaodong area is mainly composed of Archean Jiaodong Group and Early-Mesoproterozoic Jingshan Group. Among them, Jiaodong Group is the main component of the old metamorphic basement, and its lithology belongs to the Archean greenstone belt. The granite in this area is formed by the remelting of these old basement rock systems<sup>10</sup>.

Finally, according to the data in Tables 1 and 2, the author made Figure 5. For the sake of eye-catching, we projected the average value of multiple groups of data in each mineralization stage on Figure 5 (see the figure caption for more detailed information).

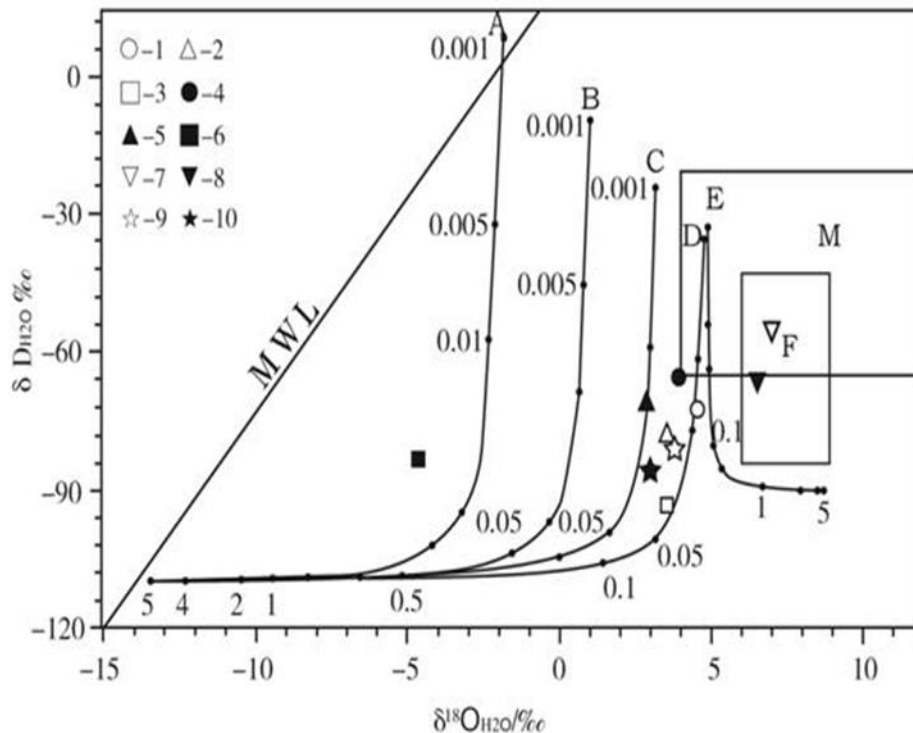


**Figure 5.**  $\delta D_{H_2O}$  -  $\delta^{18}O_{H_2O}$  relationship diagram of ore-forming fluids in each mineralization stage of the Jiaojia-type and Linglong-type gold deposits

Note: The curves A, B, C, D, E, MWL, F, and M in the figure are the same as those in Figure 3. 1 - the Jiaojia-style mineralization stage I (average value of 10 samples from 5 deposits); 2 - the Jiaojia-style mineralization stage II (average value of 18 samples from 7 deposits); 3 - the Jiaojia-style mineralization stage III (average value of 6 samples from 4 deposits); 4 - the Linglong-style mineralization stage I (average value of 6 samples from 5 deposits); 5 - the Linglong-style mineralization stage II (average value of 10 samples from 4 deposits); 6 - the Linglong-style mineralization stage III (average value of 10 samples from 5 deposits); 7 - the Jiaojia-style mineralization stage II (average value of 23 sericite samples from 5 deposits); 8 - the Linglong-style mineralization stage II (average value of 2 sericite samples from 1 deposit); 9 - the Jiaojia-style mineralization stage II (average value of 5 potassium feldspar samples from 2 deposits); 10 - the Linglong-style mineralization stage II (average value of 2 potassium feldspar samples from 1 deposit)

It can be seen from Figure 5 that:

- The projection points of the main mineralization period of Jiaojia-type and Linglong-type gold deposits are located near the atmospheric precipitation evolution curve C and D at 250 – 300 °C, which is quite different from the magmatic water evolution curve and is farther away from the magmatic water area.
- The sources of the ore-forming fluids in the mineralization stages I and II of the Jiaojia-type and Linglong-type gold deposits are basically the same, only the Linglong-type gold deposit has more atmospheric precipitation mixed in the ore-forming fluids in the mineralization stage III.
- The projection points of  $\delta D_{H_2O}$  and  $\delta^{18}O_{H_2O}$  of the potassium feldspar samples of Jingwen Mao's Jiaojia and Linglong gold deposits are also located near C and D of the atmospheric precipitation evolution curves at 250 – 300 °C, which is consistent with the results of the projection points of the 7 samples in Figure 1. It also shows that the source of the fluid that formed potassium feldspar is basically the same as the source of the ore-forming fluid in the second mineralization stage of the Jiaojia and Linglong gold deposits, which is very close to the research results of previous researchers using quartz as the target mineral, and is reasonable.
- The two projection points of  $\delta D_{H_2O}$  and  $\delta^{18}O_{H_2O}$  of the sericite samples collected by Jingwen Mao from the Jiaojia-type and Linglong-type gold mines, and the projection points of the 25 samples in Figure 1, all fall within the range of the superposition of regional metamorphic water and magmatic water, indicating that the ore-forming fluid is more likely to come from metamorphic fluid. This result is very different from the large amount of research data of previous researchers using quartz as the target mineral.

Jingwen Mao believes that the ore-forming hydrothermal fluid is the result of the mixing of mantle-derived fluid and crustal fluid<sup>1</sup>. The only possible evidence is the  $\delta D_{H_2O}$  and  $\delta^{18}O_{H_2O}$  data of sericite, but these data are completely unreliable. As mentioned above, there are a series of problems in using sericite as the target mineral to determine the  $\delta D_{H_2O}$  and  $\delta^{18}O_{H_2O}$  values of ore-forming fluids, which is wrong and will not be repeated here.

What is certain is that this error is not seen from the final result, but the root cause has been planted at the beginning.

Selecting sericite as the target mineral to determine the  $\delta D_{H_2O}$  and  $\delta^{18}O_{H_2O}$  of the ore-forming fluid is in itself a low-level common-sense mistake.

## 5 The sulfur isotope problem

When explaining the  $\delta^{34}S$  distribution characteristics of sulfides in Jiaodong gold deposits, Jingwen Mao made the following description<sup>1</sup>:

Although there are several factors responsible for mineral deposition, the change of sulfur composition in the various types of gold deposits in the Jiaodong area can be closely related to  $fO_2$ . Wang and Yan<sup>18</sup> and Wang et al.<sup>19</sup> mentioned that  $\delta^{34}S$  values of pyrite are higher in the gold deposits hosted in the large and open fracture system, and lower in those hosted in small-scale and relatively close fracture system<sup>1</sup>.

To this end, Jingwen Mao specifically quoted the “ $\delta^{34}S$  variation trend and structural relationship diagram of the Zhaoyuan-Yexian gold ore belt” (Figure 6) produced by Wang<sup>19</sup>.

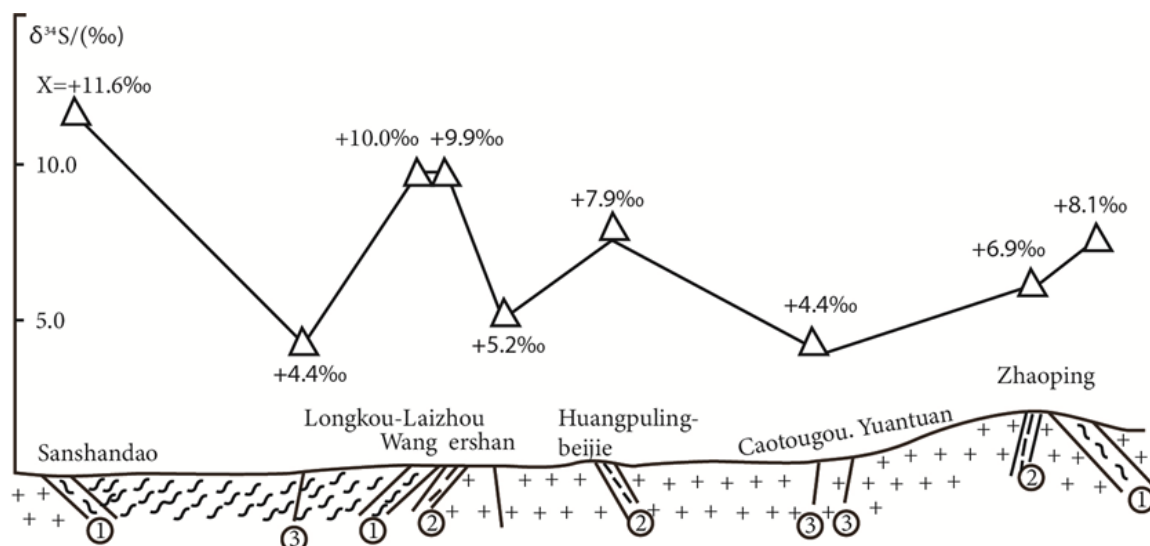


**Figure 6.**  $\delta^{34}S$  changes along the Sanshandao-Linglong gold deposits section depending on the ores-hosted fractures (Jingwen Mao quoted from Figure 4 in Wang et al's original work<sup>19</sup>)

Note: ① Regional ductile shear zone; ② Shear zone; ③ Subsidiary fracture.

Author's note of this paper: In Wang et al's original work<sup>19</sup>, ① is regional brittle-ductile-shear zone; ② is ductile shear zone; and ③ is subsidiary control fracture

Regarding this statement by Jingwen Mao, we interpret it as follows:

- In different types of gold deposits in the Jiaodong area, the changes in the sulfur isotope composition of sulfides are closely related to the oxygen fugacity  $fO_2$ .
- Pyrite formed in the tectonic background of large-scale tensional (open) fault systems (note: relatively high oxygen fugacity) has a higher  $\delta^{34}S$  value.

• Pyrite formed in the tectonic background of small-scale relatively closed fault systems (note: relatively low oxygen fugacity) has a lower  $\delta^{34}\text{S}$  value.

In short, Jingwen Mao believes that the  $\delta^{34}\text{S}$  value of sulfides and oxygen fugacity ( $f\text{O}_2$ ) are positively correlated in the Jiaodong gold mining area. This view is completely wrong and completely distorts the academic view of Wang et al.<sup>19</sup>.

According to Ohmoto's  $\log f\text{O}_2$  - pH sulfur isotope evolution diagram, namely Figure 7 in this paper (1972), when  $\delta^{34}\text{S}_{\Sigma\text{S}} = 0\text{‰}$  and  $\text{pH} \leq 7$ , the  $\delta^{34}\text{S}_{\text{Py}}$  value is basically negative. When  $\log f\text{O}_2 \geq -38$ ,  $\delta^{34}\text{S}_{\text{Py}} = -0.3$ . As  $\log f\text{O}_2$  continues to increase, the  $\delta^{34}\text{S}_{\text{Py}}$  value instantly becomes a large negative value, which can be as large as  $-24$  to  $-26$ <sup>20</sup>. Obviously, Jingwen Mao's understanding that the above-mentioned sulfide  $\delta^{34}\text{S}$  value and oxygen fugacity ( $f\text{O}_2$ ) are positively correlated is completely opposite to the research results of Ohmoto<sup>20</sup>.

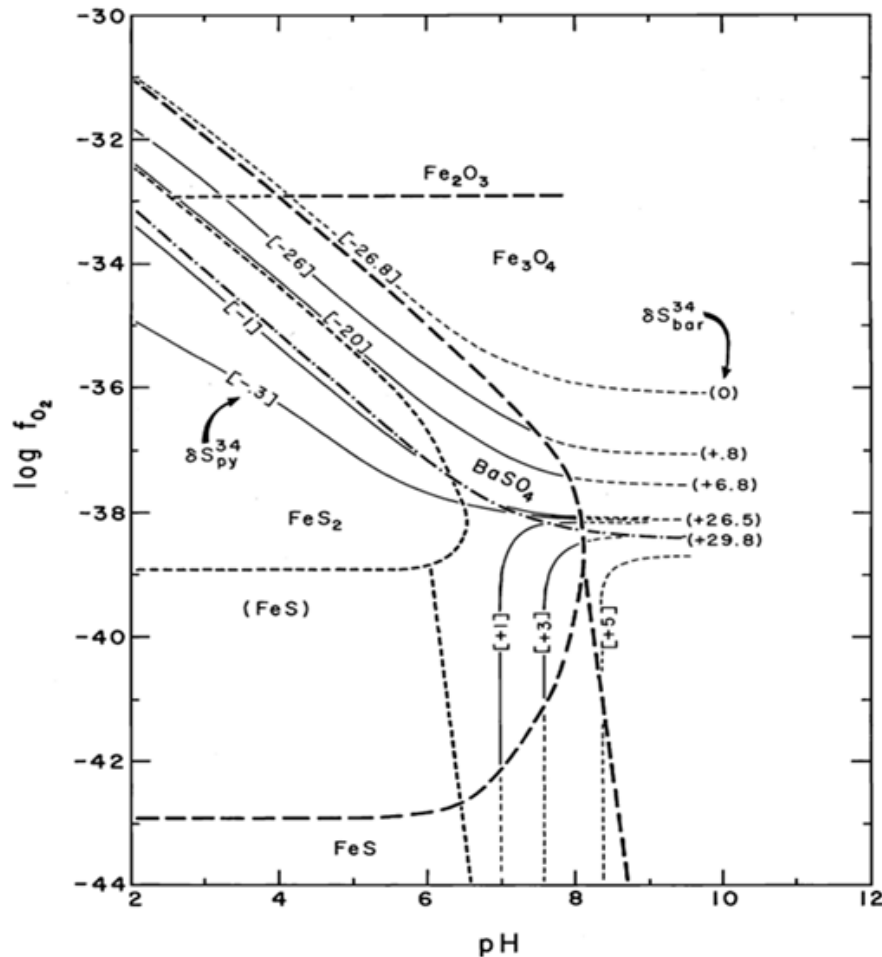


**Figure 7.** Comparison of the positions of  $\delta^{34}\text{S}_i$  contours with the stability fields of Fe-S-O minerals and barite ( $T = 250\text{ °C}$  and  $I = 1.0$ )<sup>20</sup>

Note: ~.....:  $\delta^{34}\text{S}_i$  contours. Values in [ ] and ( ) are respectively for pyrite and barite at  $\delta^{34}\text{S}_{\Sigma\text{S}} = 0\text{‰}$ ; — — —: Fe-S-O mineral boundaries at  $\Sigma\text{S} = 0.1$  moles/kg  $\text{H}_2\text{O}$ ; - - - -: Fe-S-O mineral boundaries at  $\Sigma\text{S} = 0.001$  moles/kg  $\text{H}_2\text{O}$ ; - · - · -: barite soluble/insoluble boundary at  $m_{\text{Ba}+2} \cdot m_{\Sigma\text{S}} = 10^{-4}$  (Under these  $T$  and  $I$  conditions, an increase of  $m_{\text{Ba}+2}$  or  $m_{\Sigma\text{S}}$  value by 1 order of magnitude drops the boundary by about 0.5  $\log f\text{O}_2$  units)

Wang et al. (2002) set that when  $T = 250\text{ °C}$  and  $I = 1.0$ ,  $\text{pH} = 4.3 - 7.2$ ,  $\delta^{34}\text{S}_{\Sigma\text{S}} = 10\text{‰}$ , based on the mineral paragenesis combination research and theoretical calculation, it was determined that the  $\log f\text{O}_2$  of quartz vein-type gold deposits is relatively high ( $-34$  -  $-37$ ), and the  $\log f\text{O}_2$  of altered rock-type gold deposits is relatively low ( $-34$  -  $-40$ )<sup>19</sup>.

According to the relationship between  $\delta^{34}\text{S}_{\text{py}}$  of sulfide and  $\log f\text{O}_2$ , the  $\delta^{34}\text{S}_{\text{py}}$  of pyrite in Jiaodong area ranges from 5.0‰ to 11.0‰, among which the quartz vein type gold deposit is 5.0‰ to 8.0‰, and the altered rock type gold deposit is 8.0‰ to 11.0‰. However, as the  $\log f\text{O}_2$  performance continues to increase,  $\delta^{34}\text{S}_{\text{py}}$  changes sharply towards the negative value direction. Further, under the background of overall enrichment of  $^{34}\text{S}$  in Jiaobei terrane, Wang et al. analyzed the relationship between the sulfur isotope composition of regional gold deposits and the level, mechanical properties and occurrence of ore-controlling structures based on the control of regional structure on  $\delta^{34}\text{S}$  of the ore fields. Generally, gold deposits distributed along the main fault surface or its hanging and foot walls (mainly the foot wall) in regional primary and secondary brittle-ductile shear zones with a gentle inclination (generally less than 45 degrees) are characterized by relatively enriched  $^{34}\text{S}$ . The  $^{34}\text{S}$  of gold deposits located in the third and fourth order brittle faults (mostly steep ones) far away from the main fault zone is relatively low. That is, the order and nature of the ore-controlling structure are closely related to the  $^{34}\text{S}$  of the deposit. This has resulted in the spatial pattern of alternating distribution of four  $^{34}\text{S}$  high-value zones and three  $^{34}\text{S}$  low-value zones of sulfur isotopes in the Zhaoyuan-Yexian gold deposit belt. It is based on the above research results that Wang et al. (2002) produced Figure 6<sup>19</sup>.

As shown in Figure 6, the structural belt numbered ① has four high-value  $\delta^{34}\text{S}$  belts in Sanshandao, Longkou-Laizhou, and Zhaoping area. On the contrary, the structural belt numbered ③ has three low-value  $\delta^{34}\text{S}$  belts in Tengjia, Chijia, Wasunjia, Qiansunjia, Caotouguo, and Yuantuan areas.

However, Jingwen Mao's interpretation of Figure 6 is completely opposite to Wang et al.'s<sup>19</sup>. He believes that the tectonic belt numbered ① belongs to a tensile (open) fault system, i.e., an environment with relatively high oxygen fugacity. If so, the  $\delta^{34}\text{S}$  of its sulfide should be a low-value belt, not a high-value belt. Similarly, Mao believes that the tectonic belt numbered ③ belongs to the tectonic background of a small-scale relatively closed fault system, i.e., an environment with relatively low oxygen fugacity. And under the mineralization conditions of low  $f\text{O}_2$ , the  $\delta^{34}\text{S}$  of its sulfide should be a high-value belt, not a low-value belt<sup>1</sup>. Obviously, Jingwen Mao's understanding not only violates the original intention and conclusion of Wang et al.<sup>19</sup>, but also violates the basic principle of Ohmoto (1972) on the evolution of sulfur isotopes under  $\log f\text{O}_2$  - pH conditions<sup>20</sup>.

Wang et al. also conducted more detailed research on the control of regional structure on  $\delta^{34}\text{S}$  of the ore fields<sup>19</sup>. For example, he concluded that the Jiaojia Fault Zone, which controls super-large gold deposits such as Jiaojia and Xincheng, is a brittle-ductile shear zone with a gentle dip angle, and is a regional class I ore-controlling fault zone. The fault zone was mainly plastically deformed in the early stage, and superimposed with brittle deformation in the late stage. This medium-deep semi-closed thermodynamic environment is conducive to the exchange equilibrium of sulfur isotopes, so the gold deposits controlled by this fault zone are all characterized by high  $\delta^{34}\text{S}$  values. For example, in the Linglong ore field, the Taishang gold deposit, which is located in the Potouqing Fault Zone and is controlled by the main fault surface, has a  $\delta^{34}\text{S} = 8.0\%$ , and the Fushan gold mine has a  $\delta^{34}\text{S} = 8.3\%$ .

This shows that the closer to the main fault zone (brittle-ductile shear zone) controlling the ore in the region, the greater the probability of the occurrence of altered rock-type gold deposits, and the higher the  $\delta^{34}\text{S}$  of sulfides. The quartz vein-type (Linglong-type) gold deposits in the brittle faults far away from the main fault surface in the footwall of the main fault have the lowest  $\delta^{34}\text{S}$ . The above-mentioned  $\delta^{34}\text{S}$  high-value belt (area) controlled by regional structure, from west to east, the  $\delta^{34}\text{S}$  of Sancang ore field is 11.6‰, the  $\delta^{34}\text{S}$  of Jiaoxin ore field is 9.6‰, the  $\delta^{34}\text{S}$  of Lingbei ore field is 7.9‰, the  $\delta^{34}\text{S}$  of Linglong ore field is 6.9‰, and the  $\delta^{34}\text{S}$  of Xia (dian)-Jiu (dian) ore field (southern section of Zhaoping fault) is 7.3‰.

On the contrary, the  $\delta^{34}\text{S}$  of the Tengjia and Chijia gold deposits between the Sanshandao Fault and the Jiaojia Fault is 3.7‰ - 5.8‰, which is characterized by low  $\delta^{34}\text{S}$ . The Wa Sunjia and Qian Sunjia gold deposits distributed along the secondary faults of the Jinhuaishan-Wa Sunjia fault zone between the Wangershan Fault and the Ling-Bei Fault are also characterized by low  $\delta^{34}\text{S} = 2.8\%$  - 5.3‰.

These specific data once again prove that the above academic views of Wang et al. (2002) are correct<sup>19</sup>.

Wang et al. (2002) studied the relationship between  $\delta^{34}\text{S}$  and  $\log f\text{O}_2$  of sulfides from the perspective of how redox conditions affect the conversion between  $\text{H}_2\text{S}$  and  $\text{SO}_4^{2-}$ , and pointed out that the sulfur isotopes of gold mines in the Zhaoyuan-Yexian area are characterized by rich  $\delta^{34}\text{S}$ <sup>18</sup>.

According to the analysis results of inclusion composition, the sulfur in the fluid during the mineralization period of Jinchiling gold deposit is mainly  $\text{H}_2\text{S}$ , with only trace amounts of  $\text{SO}_4^{2-}$ . In the temperature range of 150 - 300 °C, pyrite  $\delta^{34}\text{S}$  (4.75‰) basically represents the  $\delta^{34}\text{S}$  of hydrothermal fluid. The  $\delta^{34}\text{S}$  of sphalerite in Shilipu silver mine varies from -2.12‰ to -4.6‰. The reason for the decrease in sphalerite  $\delta^{34}\text{S}$  may be the increase in hydrothermal  $f\text{O}_2$  during the polymetallic mineralization stage, which leads to the transformation of  $\text{H}_2\text{S} \rightarrow \text{SO}_4^{2-}$ .

This indicates that the difference in sulfur isotopes is due to the increase in oxygen fugacity during fluid evolution, which causes part of  $\text{H}_2\text{S}$  to be converted into  $\text{SO}_4^{2-}$ , and  $\text{SO}_4^{2-}$  is enriched in heavy sulfur. For example, at 250 °C,

4% of  $\text{H}_2\text{S}$  in the hydrothermal fluid is converted into  $\text{SO}_4^{2-}$ , and the  $\delta^{34}\text{S}$  of sphalerite decreases by about 1‰ in Jinchiling Gold Mine. 20% of  $\text{H}_2\text{S}$  in the hydrothermal fluid is converted into  $\text{SO}_4^{2-}$ , and the  $\delta^{34}\text{S}$  of sphalerite decreases by about 7‰ in Shilipu Silver Mine. For another example, among the deposits in the study area, the oxygen fugacity ( $f\text{O}_2$ ) of Liukou Gold Mine is as high as -33 - -34, and its  $\delta^{34}\text{S}_{\text{py}}$  can reach as low as -14.2‰, with an average of 4.3‰ for 7 samples<sup>18</sup>. The above facts show that the  $\delta^{34}\text{S}$  of sulfides in hydrothermal endogenous metal deposits is closely related to the oxygen fugacity ( $f\text{O}_2$ ) under mineralization conditions, but it is not a positive correlation, but a reverse increase and decrease.

Jingwen Mao consulted the paper by Wang et al. (2002)<sup>19</sup>, but he did not understand it. In order to explain the distribution characteristics of  $\delta^{34}\text{S}$  of sulfides in the Jiaodong gold mining area, which has four high-value bands and three low-value bands as shown in Figure 6, Jingwen Mao not only completely reversed right and wrong, but also attributed this error to Wang<sup>18</sup> and Wang et al.<sup>19</sup>. This is not only an unethical academic behavior, but also shows that Jingwen Mao does not understand the basic knowledge of sulfur isotope geochemistry.

Sulfur isotopes are one of the important means to study the source of ore-forming materials and the genesis of ore deposits. The relevant contents discussed by Ohmoto, Wang, and Wang etc. should be familiar to ore geologists<sup>18-20</sup>. But Jingwen Mao turned right and wrong upside down. In the field of scientific research, such behavior of pretending to know is intolerable.

What is even more despicable is that Jingwen Mao linked his own erroneous views with Wang et al.<sup>18</sup>. For this reason, we consulted Wang et al.'s paper<sup>18</sup>. In their paper, Wang et al. did not mention any relationship between the  $\delta^{34}\text{S}$  value of sulfides and ore-controlling structures in the Jiaodong gold mining area. Jingwen Mao completely fabricated and imposed his views on others.

## 6 Conclusions

As can be seen from the above discussion, in order to determine the source of the ore-forming fluid of the Jiaodong gold deposit and explore the genesis of the deposit, Jingwen Mao chose sericite as the target mineral, extracted water from sericite by crushing, and determined the hydrogen and oxygen isotope composition of the ore-forming fluid, which is completely wrong.

In the absence of the oxygen isotope fractionation coefficient relationship between sericite and water, Jingwen Mao used the oxygen isotope fractionation coefficient relationship between muscovite and water instead, which is a mistake on top of a mistake.

When explaining the relationship between the high and/or low changes in the  $\delta^{34}\text{S}$  values of sulfides in different types of Jiaodong gold deposits and  $\log f\text{O}_2$ , Jingwen Mao believed that the high or low changes in the  $\delta^{34}\text{S}$  values of sulfides were positively correlated with  $\log f\text{O}_2$ , which completely contradicted the research results of Ohmoto.

In the field of stable isotope geochemistry, Jingwen Mao's paper with frequent errors was published in *Ore Geology Reviews*, which had a wide impact and a very bad effect. As an ore geologist, he made such a low-level mistake in such a conventional research field, which is a shame for the Chinese geological community.

Science pursues truth as its ultimate goal, and scientists take benefiting mankind as their responsibility. This sacred mission does not tolerate any form of fraud, pretending to know, or making up stories. This bad behavior that is completely contrary to the professional ethics of scientific workers must be exposed.

The author has not conducted any research on the Jiaodong gold mine, but the purpose of this article is to clarify matters and get to the bottom of things.

## 7 References

1. Mao JW, Wang YT, Li HM, Pirajno F, Zhang CQ & Wang RT. 2008. The relationship of mantle-derived fluids to gold metallogenesis in the Jiaodong Peninsula: Evidence from D–O–C–S isotope systematic. *Ore Geology Reviews*, 33: 361–381.
2. Ohmoto H & Rye OR. 1974. Hydrogen and oxygen isotope compositions of fluid inclusions in the Kuroko deposits, Japan. *Econ. Geol.*, 68: 947-953.
3. Wang DZ (ed.). 1965. *Optical Mineralogy*. Shanghai: Shanghai Science and Technology Press. pp 370 (in Chinese).
4. <https://en.wikipedia.org/wiki/Sericite>. Retrieved January 31, 2021.
5. <https://www.britannica.com/science/paragonite>. Retrieved January 31, 2021.
6. <https://www.britannica.com/science/mica>. Retrieved February 6, 2021.
7. Zheng YF & Chen JF. 2000. *Stable isotope geochemistry*. Beijing: Science Press. pp316 (in Chinese with English abstract).
8. Wang ZK. 1991. Characteristics of lead, hydrogen and oxygen isotopes in the Qixia gold deposit in Jiaodong and their genetic significance. *Journal of Tianjin Geological Society*, 9 (3): 45-49 (in Chinese).



9. Li ZP. 1992. Genesis of the Rushan gold deposit in Jiaodong. *Mineral Deposit Geology*, 11 (2): 165-187 **(in Chinese with English abstract)**.
10. Li ZL & Yang MZ. 1993. *Geology and Geochemistry of Jiaodong Gold Deposits*. Tianjin: Tianjin Science and Technology Press. pp 300 **(in Chinese with English abstract)**.
11. Zhang LG, Chen ZS & Liu JX. 1994. Water-rock exchange in Jiaojia-type gold deposits: a study on the hydrogen and oxygen isotope composition of ore-forming fluids. *Mineral Deposits*, 13 (3): 193-200 **(in Chinese with English abstract)**.
12. Zhang LG. 1985. *Application of stable isotopes in geological science*. Xian: Shaanxi Science and Technology Press. pp.386 **(in Chinese with English abstract)**.
13. Li ZL. 1989. Stable isotope geochemical characteristics of gold deposits in the Jiaodong area and their relationship with gold deposits. In: *Proceedings of the International Symposium on Gold Geology and Exploration*. Shenyang: Northeast Polytechnic University Press. pp. 519-520 **(in Chinese with English abstract)**.
14. Zhai JP, Xu GP & Hu K. 1998. Mineral fluid and isotopic characteristics and significance of the Qixia gold deposit. *Mineral Deposits Geology*, 17 (4): 307-318 **(in Chinese with English abstract)**.
15. Zhai JP, Hu K & Lu JJ. 1996. Study on the lamprophyre and fluids, oxygen and strontium isotopes in the Rushan gold deposit. *Mineral Deposits*, 15 (4): 358-364 **(in Chinese with English abstract)**.
16. Lu HZ, Yuan WC & Zhang GP. 1999. Stable isotopes and isotope chronology of the main gold deposits in Linglong-Jiaojia area. *Journal of Gullin Institute of Technology*, 19 (1): 174-188 **(in Chinese with English abstract)**.
17. Wang BC, Xu JF & Zheng WS. 1995. Ammonia, hydrogen, oxygen stable isotope geochemistry and deposit genesis of some gold deposits in Jiaodong area of Shandong Province. *Precious Metal Geology*, 4 (1): 25-34 **(in Chinese with English abstract)**.
18. Wang TJ & Yan F. 2002. Evolution of ore-forming fluids and mineralization prediction of magmatic hydrothermal gold deposits in the Jiaodong area. *Journal of Geological Prospecting*, 17 (3): 169-174 **(in Chinese with English abstract)**.
19. Wang YW, Zhu F & Gong RT. 2002. Tectonic isotope geochemistry: a further study of sulfur isotopes in the concentrated gold deposits of Jiaodong. *Gold*, 23 (4): 1-16 **(in Chinese with English abstract)**.
20. Ohmoto H. 1972. Systematics of sulfur and carbon isotopes in hydrothermal ore deposits. *Econ. Geol.* 67: 551-578.





## Original Article

**Indium use, resource, market and ore deposit type**JZ Yin<sup>1,2,3</sup> **Abstract**

With the continuous advancement of science and technology, rare dispersed elements that have long been dormant in rocks and ignored by humans have become increasingly important. Indium is one of these rare dispersed elements, although most people know little or nothing about it. In fact, indium has a wide range of important uses in many aspects. Given the unique physical and chemical properties of indium, some uses are even irreplaceable. Therefore, many countries have included some rare elements, including indium, in the list of national strategic resources or critical metals for protection. This article not only popularizes the main uses of indium in modern society, briefly describes the distribution and current status of natural indium ore resources around the world, but also explores its market status in the past 10 years and future development trends. Finally, the main genesis types of associated or symbiotic indium ores around the world are summarized and briefly discussed. Because indium does not exist as an independent deposit and can only exist as a by-product of non-ferrous metals such as copper, lead, zinc and tin, it is very important to research and develop new sources of indium, including recycling and reuse. These new sources include but are not limited to waste rock piles and tailings from related abandoned old mines, etc.

**Key words:** Rare dispersed metal indium; use; global resource distribution; market and trend; origin type

---

**Affiliation Info:** <sup>1</sup> Orient Resources Ltd., Canada; <sup>2</sup> Wuhan Institute of Technology, Wuhan 430205, China; <sup>3</sup> College of Earth Sciences, Jilin University, Changchun 130061, China

**Article Info:** Received: 18 May 11, 2024 / Revised: 30 May 2024 / Accepted: 16 June 2024 / Published Online: 30 June 2024. [www.naturalisscientias.com](http://www.naturalisscientias.com)

**Authors' Contact Info:** Yin, JZ: [jimyin7@yahoo.ca](mailto:jimyin7@yahoo.ca)

**Citation:** Yin, JZ. 2024. Indium use, resource, market and ore deposit type. *Naturalis Scientias*, 1 (2): 152-166. DOI: <https://doi.org/10.62252/NSS.2024.1011>.

**Copyright** © 2024 by the authors. Published by *Naturalis Scientias*. This is an open access article under the Creative Commons Attribution-NonCommercial 4.0 International (CC BY-NC 4.0) License. (<https://creativecommons.org/licenses/by-nc/4.0/>).

**Corresponding Author** : Yin, JZ, PhD, PGeo, Professor; Email: [jimyin7@yahoo.ca](mailto:jimyin7@yahoo.ca)

## 1 Introduction

With the rapid development and continuous progress of science and technology, many metals that were not noticed by people, especially those rare metals have been constantly entering people's sight, gaining more and more attention, and playing an indispensable and important role in modern industries. Most of the rare dispersed elements that ordinary people don't know about are an important category of these metals.

Most people are familiar with bulk mineral products such as steel, aluminum alloys and various copper alloys that are closely related to their daily lives, but few people know about rare metals such as indium (In), gallium, rhenium, etc. In fact, the indium mentioned here is one of the many rare dispersed elements.

This article will analyze the distribution and production status of global indium resources on the basis of introducing the main uses of indium, a rare metal in modern life, and then explore the market and future trends of indium products, and then classify its deposit genesis types. In the future, another article will discuss its formation conditions, etc.

## 2 Use

Indium is a soft, silvery-white metal with a slightly bluish tint. Pure indium metal is highly plastic and will leave marks if you squeeze it gently. It can also be easily pressed into slices or cut into blocks, just like the tofu we often see in our daily lives. Indium metal has a low melting point and electrical resistance, but a high boiling point. It has excellent ductility, plasticity, and corrosion resistance. In addition, indium has excellent light permeability and electrical conductivity, making it one of the best semiconductor materials<sup>1-3</sup>.

Indium is located in the fifth period and group IIIA of the periodic table. It has an atomic weight of 114.818 and is the 49th element. The average abundance of In in the continental crust is 0.052 ppm where it is nearly always found as a trace element in other minerals<sup>4</sup>. Obviously, the content of In in the earth's crust is low and very dispersed, and it only exists as an impurity in metal deposits such as zinc and lead. Therefore, people classify indium as a rare metal together with elements with similar characteristics such as gallium, thallium, germanium, selenium, tellurium and rhenium. The chemical properties of indium are between those of gallium and thallium. In 1863, Ferdinand Reich and Hieronymus Theodor Richter discovered indium through spectroscopy and named it indium because of its indigo spectral line. However, it was not until the following year that indium was successfully isolated. The special physical and chemical properties of indium determine that there is no elementary substance indium in nature. Indium generally exists in combination with other elements to form related compounds.

Due to its low melting point, high boiling point, good ductility, strong plasticity, low resistance, good superconductivity and corrosion resistance, as well as good light permeability and conductivity, indium is widely used in high-tech fields such as radio and electronic industry, aerospace, alloy manufacturing, new materials for solar cells, medical, national defense and military, high-tech, nuclear industry, modern information industry and energy. Indium is also commonly found in the display screens of computers and smartphones that modern humans almost cannot live without. ITO targets used in the production of liquid crystal displays and flat-panel screens are the main consumer of indium ingots, accounting for about 70% of global indium consumption. The second largest consumer is the electronic semiconductor field, which accounts for about 12% of global consumption. Indium consumed in the solder and alloy field accounts for about 12%. The scientific research industry consumes about 6% of indium (Figure 1)<sup>1-3, 5</sup>.

Metal indium was originally used to manufacture industrial bearings and has been used ever since. After the surface of the bearing is plated with indium, its service life is extended by 5 times that of the bearing with ordinary coating. The alloy of indium and gallium can lubricate the sliding elements, so it is used in electric vacuum instruments.

Indium is easy to form a firm coating on the metal surface and has good corrosion resistance. Especially, it can prevent the corrosion of alkaline solution to the metal. The coating of indium not only has a bright color but also is easy to polish. In addition to pure indium coating, alloys such as indium and zinc can also be used as coatings. Indium coating is also used in decorative crafts. When the surface of various mirrors, retroreflectors and reflectors is plated with indium, its reflective performance will be greatly enhanced and resistant to seawater erosion. Therefore, this coating is often used in the reflectors of ships. In addition, bronze mesh with indium coating on the surface can be used to remove mercury vapor in vacuum instruments.

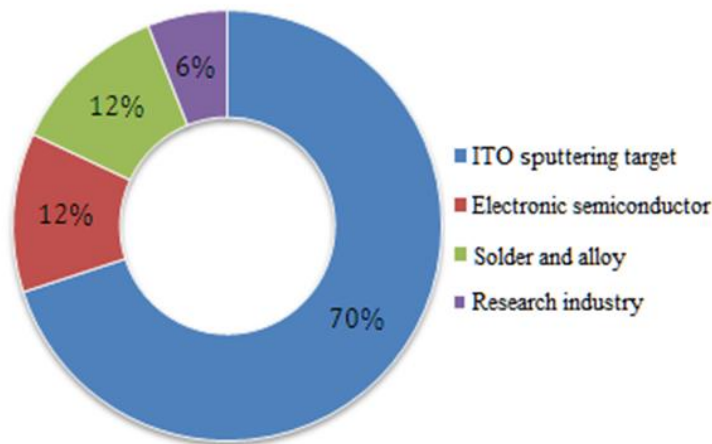


**Figure 1.** The main uses of indium and their proportion<sup>2</sup>

Because indium has a low melting point, it can be used to manufacture a variety of fusible alloys. This type of indium-containing alloy with a melting point in the range of 47 to 122 °C is mostly used to manufacture various types of fuses, fuse cutouts, thermostats and signal devices.

Many fusible alloys of indium can be used as brazing materials. Indium and its alloys can firmly weld parts made of piezoelectric materials together. When making multi-layer integrated circuits, it is crucial to choose brazing materials containing indium.

The glassy composite of high-purity indium oxide and tin oxide (ITO) is used to make transparent conductive electrodes in the plasma TV and LCD TV screen industries, and is also used as a sensitive element for measuring certain gases. In the radio and electronics industries, indium and silver oxides are mixed and pressed into special contact devices. Many alloys can improve their strength, ductility; wear resistance and corrosion resistance after adding a small amount of indium. Indium has also earned the reputation of "vitamin of alloys", and some people call it the "wonderful indium effect".

Indium alloys can be used to produce solar cells. The new generation of copper-indium-gallium-selenium (CIGS) thin-film solar cells has the characteristics of low production cost, low pollution, no decay, and good weak light performance. More importantly, the photoelectric conversion efficiency of this cell ranks first among various thin-film solar cells, close to crystalline silicon solar cells, but its cost is only one-third of the latter. Therefore, it is called "a very promising next-generation new thin-film solar cell" by the international community. This cell also has a soft, uniform black appearance, which is an ideal choice for places with high requirements for appearance, such as glass curtain walls of large buildings.

Indium is also the core material for manufacturing computer chips and indium tin oxide (ITO). Adding a very small amount of indium can greatly improve the performance of related products.

Indium is also one of the important basic materials that are indispensable for modern high-tech weapons and equipment. Since the 1980s, the U.S. Defense Logistics Agency (DLA) has included indium in the list of national defense reserve materials. In modern military high technology, indium is mainly used in electronic and information equipment. From military command to weapon guidance, from television to electronic countermeasures, components containing rare metals such as indium are used. The infrared imager that relies on the different thermal radiation of the target and the background to form an image is an infrared photoelectric system. When combined with other devices, it becomes a multi-sensor intelligent system and an all-weather, all-day combat tool. According to relevant materials, the United States has equipped the military with at least more than 100 types of thermal imagers. The "eyes" of the infrared thermal imager are infrared detectors, and the main materials used are CdSb, InSb, and InAsSb/Si, etc. The newer generation of infrared detectors under development will use InSb components. This component has higher sensitivity and resolution, and a longer use distance<sup>1-3, 5-7</sup>.

Because indium is an indispensable rare resource in many high-tech fields such as the above, it has been listed as a critical mineral by China, the European Union, the United States, Japan and other countries. The so-called critical mineral means that foreign investors cannot get involved in the exploration and development of this mineral resource. The import and export of related mineral products are also strictly controlled by relevant countries.

Due to its good ductility and plasticity, low vapor pressure, and ability to adhere to a variety of materials, indium is also widely used as a gasket or lining material in high-altitude instruments and aerospace equipment. Indium foil is often used as a contactor for ultrasonic linear blocking. In the atomic energy industry, indium is used to make neutron indicators. Many indium alloys are often used to make control rods in nuclear reactors. Indium is also an excellent material for making neutron detectors, comparable to metallic gallium.

In addition to the above application fields, one of the more promising application fields of indium is the field of oral medicine. It is known that alloys used for dentures are basically alloys with gold, silver and palladium as main components and 0.5% to 10% indium added. Adding a small amount of metallic indium to the material of dental prostheses can significantly improve the corrosion resistance and hardness of these prostheses, and this alloy material will not turn black<sup>1-3, 5-6</sup>.

According to relevant analysis, the amount of indium used in new applications is still increasing at a rate of 10 % - 20 % per year<sup>2-3, 5-10</sup>.

In German, some resources are called Gewürzmetall (spice metals) because, like spices such as cinnamon or saffron, they only account for a small proportion of the production process of electronic devices, but are essential for certain functions.

Indium is one of these spice metals.

### 3 Resource

Similar to many other mineral resources on the earth's surface, the distribution of indium ore deposits on this planet is also extremely uneven (Figure 2). Not only is the overall resource volume of indium ore relatively small, but it is also mainly concentrated in a few countries such as China, Peru, the United States, Canada and Russia. Among them, China has the richest indium ore resources, accounting for about 72.0 % of the global total. Peru has the second largest indium resources in the world, accounting for about 3.3% of the world's total. The United States ranks third, accounting for about 2.5% of the global total (Figure 3)<sup>8-10</sup>.

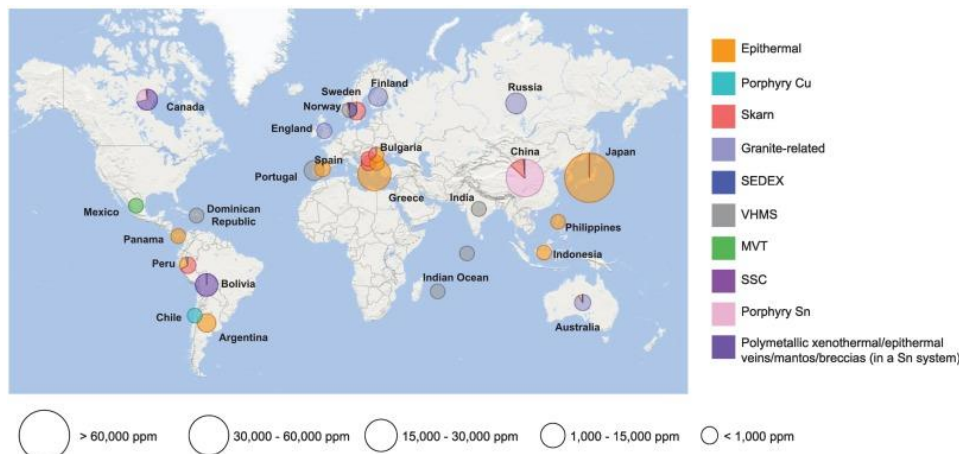


**Figure 2.** Map of the average indium content of indium-bearing minerals per mineralization style and by country<sup>11</sup>

The bubble size corresponds to the visual representation of the relative indium content in ppm measured by EPMA or LA-ICP-MS Abbreviations VHMS: volcanic-hosted massive sulfide deposits; SEDEX: sedimentary exhalative mineral deposits; SSC: sediment-hosted stratiform Cu; MVT: Mississippi Valley-type Zn-Pb

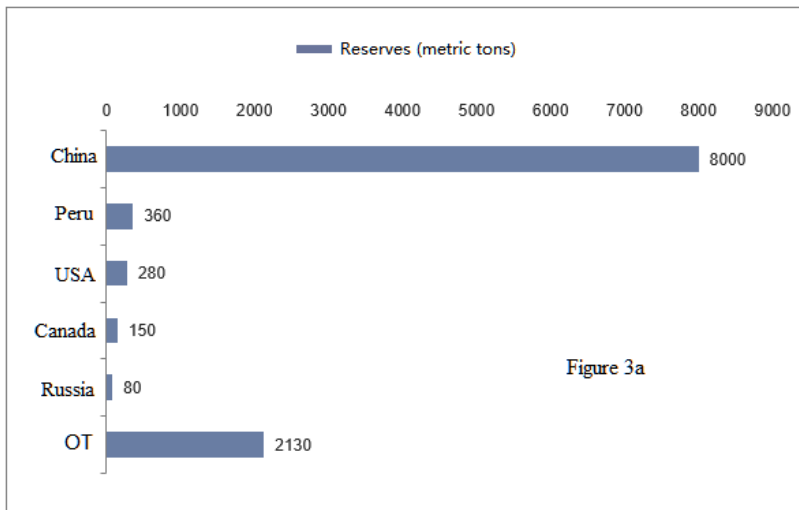
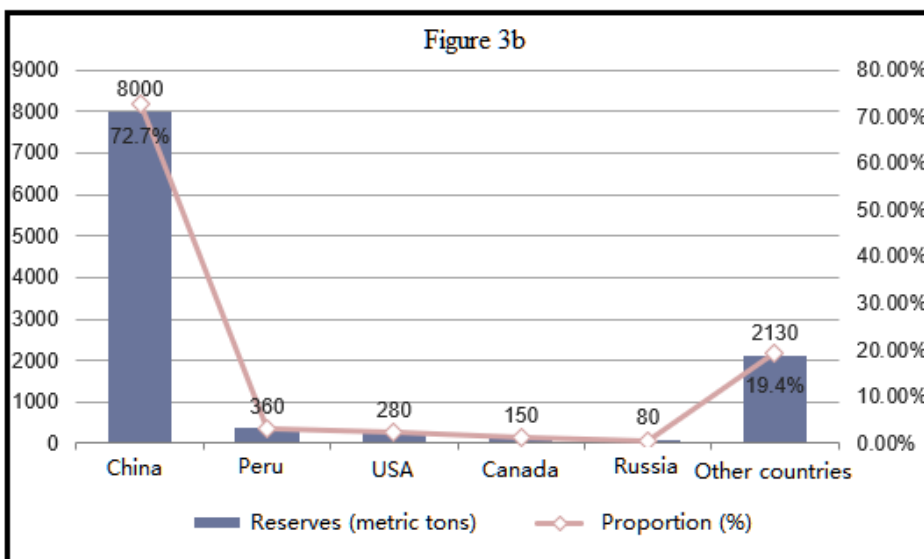


Figure 3a

Figure 3a & 3b. Indium reserves (a & b) and percentages (b) of major countries around the world<sup>8-10</sup>

According to statistics from relevant departments of the China Ministry of Natural Resources, China's indium reserves in 2021 were 1,998.7 tons, an increase of 11.5% from 1,792.77 tons in 2020. From the perspective of administrative divisions, China's indium resources are mainly concentrated in the following provinces (Figure 4): In 2021, the indium reserves in Guangxi accounted for 68.9% of the country's total, or 1,377.38 tons. Other provinces such as Inner Mongolia, Jiangxi, Yunnan and other places also have relatively high indium reserves.

For a long time, all rare dispersed elements, including indium, have been sentenced to death by traditional geochemistry and mineral geology theory: because their abundance in the earth's crust is too low, they cannot form their own independent primary deposits, and can only appear as associated elements in traditional bulk ores such as copper, lead and zinc.

It was not until the first half of the 1990s that this death sentence on rare dispersed elements was broken by the discovery of the Dashuigou independent tellurium deposit on the southeastern edge of the Qinghai-Tibet Plateau. It turns out that under special geological settings, some rare elements can form independent primary deposits<sup>12-19</sup>.

But the musty old death sentence of conventional mineral deposit geology still applies to all other rare dispersed elements except tellurium, including the subject of this article, indium. The fact is that almost all the indium in the world today comes from zinc minerals. To date, no isolated and independent indium deposit has been discovered.

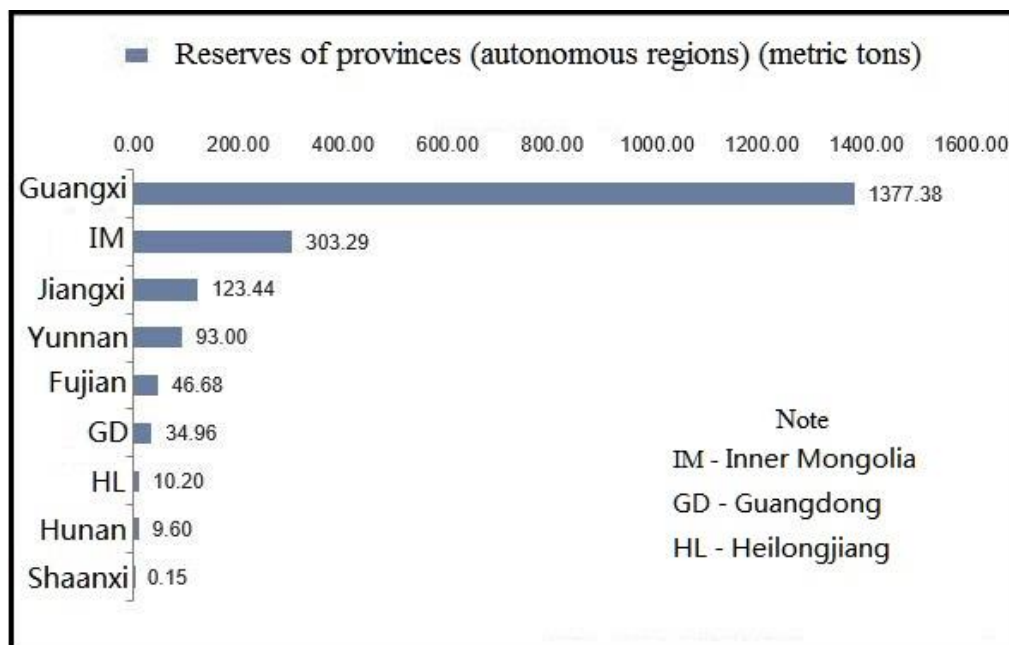


Figure 4. Statistical ranking of indium ore reserves in China's provinces (autonomous regions) in 2021<sup>8-10</sup>

#### 4 Market

At present, there are two main sources of refined indium products. According to different extraction sources, refined indium products can be divided into primary indium and recycled indium. The main raw materials of primary indium are crude zinc, crude lead, slag, smoke, alloy, anode mud, leached slag and related solutions obtained after smelting of indium-containing concentrates such as sphalerite and galena. Recycled indium is recovered and refined from discarded ITO targets and indium-containing semiconductor waste, discarded parts, alloy processing waste, waste catalysts and other materials. In addition, it also includes the recycling and refining of discarded indium-containing terminal products.

At present, the main extraction process and mainstream extraction process technology for refined indium production in the world is extraction-electrolysis. Its principle process flow is: indium-containing raw materials → enrichment → chemical dissolution → purification → extraction → stripping → zinc (aluminum) replacement → sponge indium → electrolytic refining → refined indium.

China not only has the world's largest amount of primary indium resources, but is also the world's largest producer and exporter of primary indium products, accounting for more than 30% of the world's total indium production. The so-called primary indium products refer to refined indium ingots derived from primary indium ore with a purity of 99.995% or more<sup>8-10</sup>.

According to Mineral Commodity Summaries released by the U.S. Geological Survey in January 2023<sup>21</sup>, China, the leading producer and exporter of indium globally, exported 421 tons of indium in the first 8 months of 2022, a 13% increase compared with exports in the same period in 2021 (Table 1). Exports were primarily sent to the Republic of

Korea, 55%; Singapore, 14%; and Hong Kong, 12%. Some zinc smelters in Sichuan and Yunnan Provinces in China temporarily cut production during the year in response to power supply issues, according to news sources; however, the extent of the cuts and their effect on related byproduct metal production, including indium, could not be quantified.

**Table 1.** Estimated world refinery production of indium<sup>21</sup>

Country/Year	2021	2022
United States	n/a	n/a
Belgium	20	20
Canada	60	55
China	540	530
France	38	20
Japan	66	66
Republic of Korea	190	200
Peru	12	n/a
Russia	5	5
Uzbekistan	1	1
World total (rounded)	932	900

An indium-producing zinc smelter in Aubry, France, was placed on care-and-maintenance status in January owing to high power prices. The smelter resumed production at a reduced rate in March. Annual indium production at the smelter was last reported in 2018 at 43 tons<sup>21</sup>.

In this concise summary of indium, USGS emphasizes that indium is most commonly recovered from the zinc-sulfide ore mineral sphalerite. The indium content of zinc deposits from which it is recovered ranges from less than 1 part per million to 100 parts per million. Although the geochemical properties of indium are such that it occurs in trace amounts in other base-metal sulfides—particularly chalcopyrite and stannite—indium recovery from most deposits of these minerals was not economic. This seems to imply that indium ore resources are indeed limited and not inexhaustible. Humans are urged to use and cherish them.

Finally, USGS specifically said this in a short paragraph about indium substitutes: Antimony tin oxide coatings have been developed as an alternative to ITO coatings in LCDs and have been successfully annealed to LCD glass; carbon nanotube coatings have been developed as an alternative to ITO coatings in flexible displays, solar cells, and touch screens; poly (3,4-ethylene dioxythiophene) (PEDOT) has also been developed as a substitute for ITO in flexible displays and organic light-emitting diodes; and copper or silver nanowires have been explored as a substitute for ITO in touch screens. Graphene has been developed to replace ITO electrodes in solar cells and also has been explored as a replacement for ITO in flexible touch screens. Researchers have developed a more adhesive zinc oxide nanopowder to replace ITO in LCDs. Hafnium can replace indium in nuclear reactor control rod alloys<sup>21</sup>.

This is obviously good news. It means that we are encouraged not to lose confidence because of the limited natural indium resources mentioned above. After all, science and technology have been developing and scientific and technological workers will always find substitutes for natural rare substances such as indium to make human life and future better.

Thanks to the substantial increase in indium production in China and South Korea, global primary indium production has gradually increased since 2010, reaching a peak of 844 tons in 2014. Then it gradually declined. In recent years, production has gradually recovered and reached 760 tons in 2019, a year-on-year increase of 2.6%<sup>8-10</sup>.

In terms of specific national production, Japan's primary indium production in 2019 was 75 tons, a year-on-year increase of 7.1%. Canada's primary indium production was 60 tons, a year-on-year increase of 3.5%. Belgium, Peru and Russia's primary indium production was 20, 10 and 5 tons respectively<sup>8-10, 22</sup>.

South Korea is one of the countries that is worthy of attention in producing primary and recycled indium. In recent years, South Korea has maintained a high production capacity of refined indium. Relying on its status as one of the world's major consumers and the world's second largest zinc smelting capacity, South Korea's production of recycled and primary indium has grown rapidly. As of 2019, South Korea's primary indium production was 240 tons, a year-on-year increase of 2.1%. The raw materials for primary indium in South Korea mainly come from refined zinc ore in Bolivia.

China is not only the country with the richest indium reserves in the world, but also the world's largest producer of primary indium. From 2010 to 2014, China's primary indium production increased at an average annual rate of 8.8%. In 2015, due to the bankruptcy of the Pan Asia Nonferrous Metals Exchange, China's indium market showed a serious oversupply situation, and the price of indium plummeted, causing a sharp decline in indium production, a year-on-year decrease of 23.9%. After that, it continued to decline year by year, and it did not rise until 2018 to 300 tons, accounting for 39.5% of the world. As of 2019, China's primary indium production remained at 300 tonnes, the same level as in 2018<sup>8-10, 22</sup>.

As far as global indium production is concerned, with the continuous growth of demand for downstream panels from 2015 to 2019, global indium production continued to grow. In 2020-2021, due to the overall demand and the impact of the epidemic on global trade, the overall indium supply fell slightly, with production in 2020 and 2021 being 957 tons and 920 tons respectively.

As for the overall consumption of indium, although the United States has a certain amount of indium reserves, its overall indium consumption comes from imports. Data show that the United States imported 115 tons of indium in 2020. According to USGS estimates, the country's consumption in 2021 is about 170 tons (Figure 5). In terms of the main sources of imports, the United States mainly imported from China, Canada, South Korea and France from 2017 to 2020, accounting for 31%, 23%, 20% and 9% respectively (Figure 6). It is not ruled out that the strategic United States will temporarily cover up the development of domestic indium deposits and consume foreign indium products first. After all, non-renewable mineral resources will only become less and less and more expensive, not more and more cheap. Even if there are more and more alternative products to indium in the future, they cannot completely replace indium itself with unique chemical and physical properties.

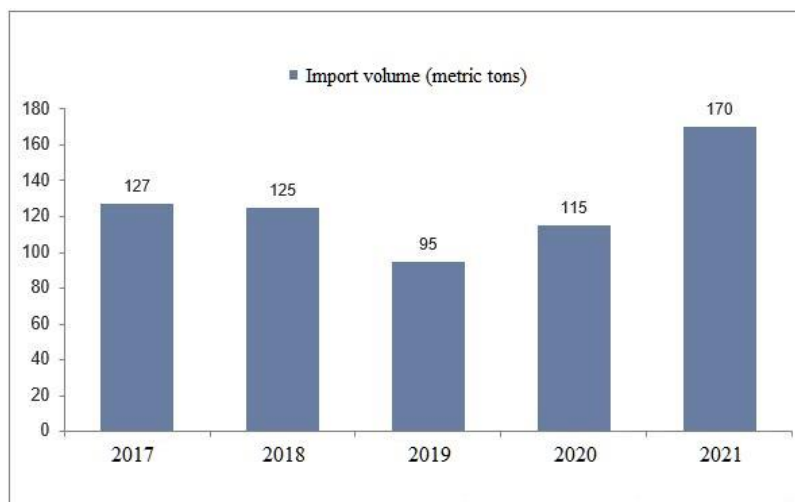


**Figure 5.** Trend of U.S. indium imports from 2017 to 2021<sup>8-10</sup>

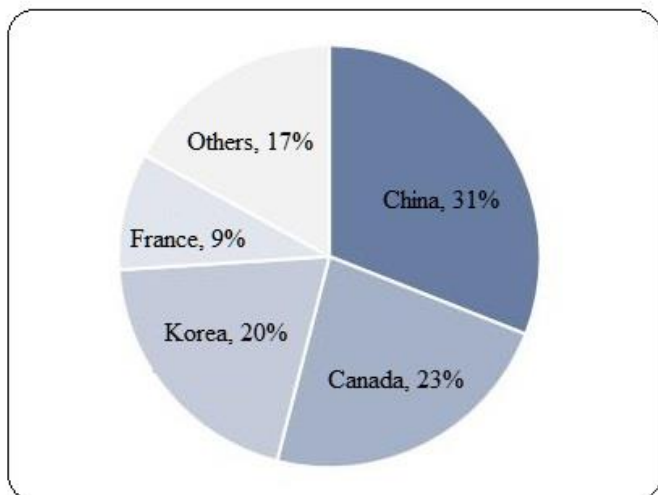


**Figure 6.** Source countries and proportions of U.S. indium imports from 2017 to 2020<sup>8-10</sup>

Driven by both exports and domestic demand, China's overall indium production has shown a steady growth trend. It reached 540 tons in 2020 and fell slightly to 530 tons in 2021.

From January to November 2022, China's indium product exports totaled 542,364 kilograms, a year-on-year increase of 13.99%. Among them, unwrought indium was 537,052 kilograms, a year-on-year increase of 13.51%; wrought indium was 5,312 kilograms, a year-on-year increase of 100.83% (Figure 7). In 2022, China exported the largest number of indium products to South Korea, Hong Kong of China, Singapore, Japan and the United States, accounting for 56.05%, 12.79%, 10.77%, 4.90% and 4.67% of the cumulative exports from January to November of that year, respectively, accounting for a total of 89.18% (Figure 8). The reason why South Korea has become the largest trading country for China's indium product exports is mainly due to China's Guangdong Province's processing trade, general trade and imported processing trade with South Korea.

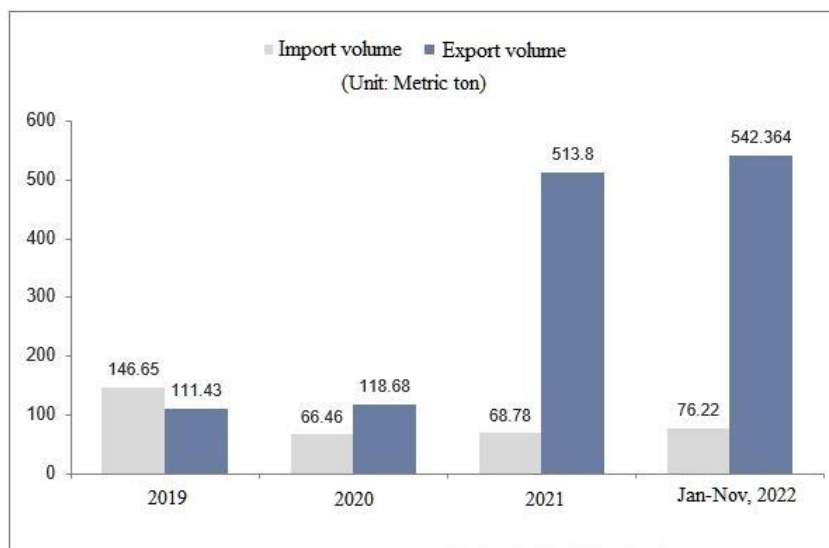


**Figure 7.** China's indium product import and export trends from November 2019 to November 2022<sup>9-10</sup>

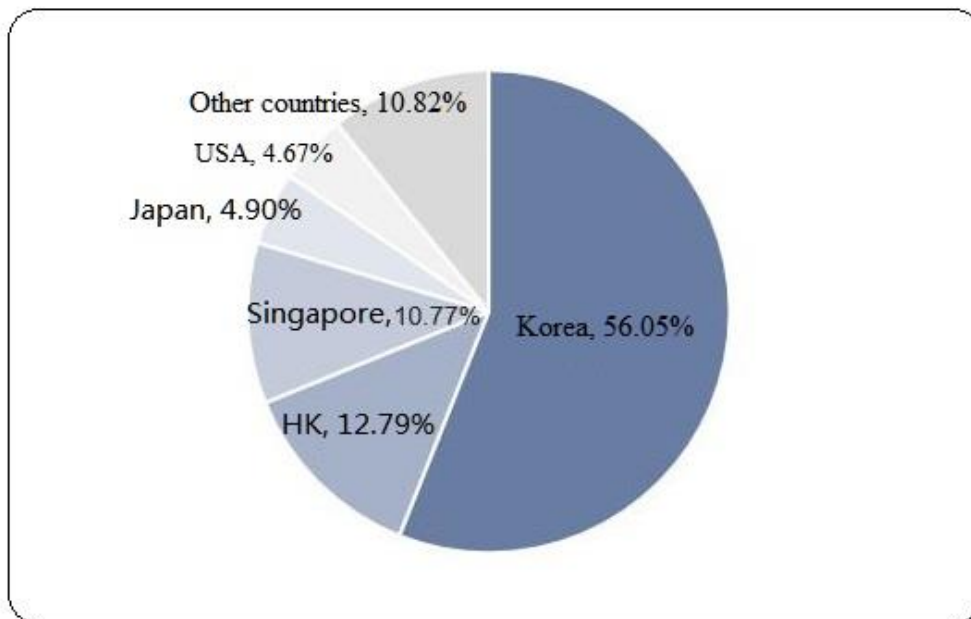


**Figure 8.** Proportion of China's indium product export destinations from January to November 2022<sup>9-10</sup>

In terms of imports, China imported a total of 76,222 kg of indium products from January to November 2022, an increase of 18.55% year-on-year. Among them, unwrought indium was 72,271 kg, a year-on-year increase of 35.17%; wrought indium was 3,951 kg, a year-on-year decrease of 63.51%<sup>8-10</sup>. Among them, China imported the largest number of indium products from Japan, South Korea, Germany and the United States, and the five countries accounted for a total of 99.07%. The largest share of this is from Japan, which accounts for 44.6%, and the main importer is Yunnan, China, which imports unwrought indium from Japan (Figure 7).

Since 2022, the production space of refined indium products in China has not changed much. Hunan, Guangxi, Guangdong and Yunnan are still the main production areas, but the ranking of enterprises has changed greatly. During this period, China's refined indium production increased to 667 tons, an increase of 12.1% in 2022 compared with 2021. Among them, primary indium increased by 3% and recycled indium increased by 35.5%<sup>8-10, 22</sup>.

In 2022, China's domestic refined indium consumption was about 496 tons, an increase of 6.2% over 2021. This increase in indium consumption is mainly due to the breakthrough in indium target manufacturing technology and the expansion of mass production scale. In 2022, China's domestic ITO target consumption reached 436 tons, an increase of 5.6% over 2021, accounting for about 87.9% of the overall domestic refined indium consumption.

Some studies believe that with the continuous improvement of the degree of localization, the growth rate of China's target production will continue to accelerate, and it is expected that the indium consumption in this field will exceed 500 tons in 2023. At present, indium targets are mainly used in the panel industry.

Since 2018, due to the overall sluggish demand, the domestic indium price in China has generally shown a downward trend (Figure 9). By the end of 2019, it was only around RMB 900 per kg.

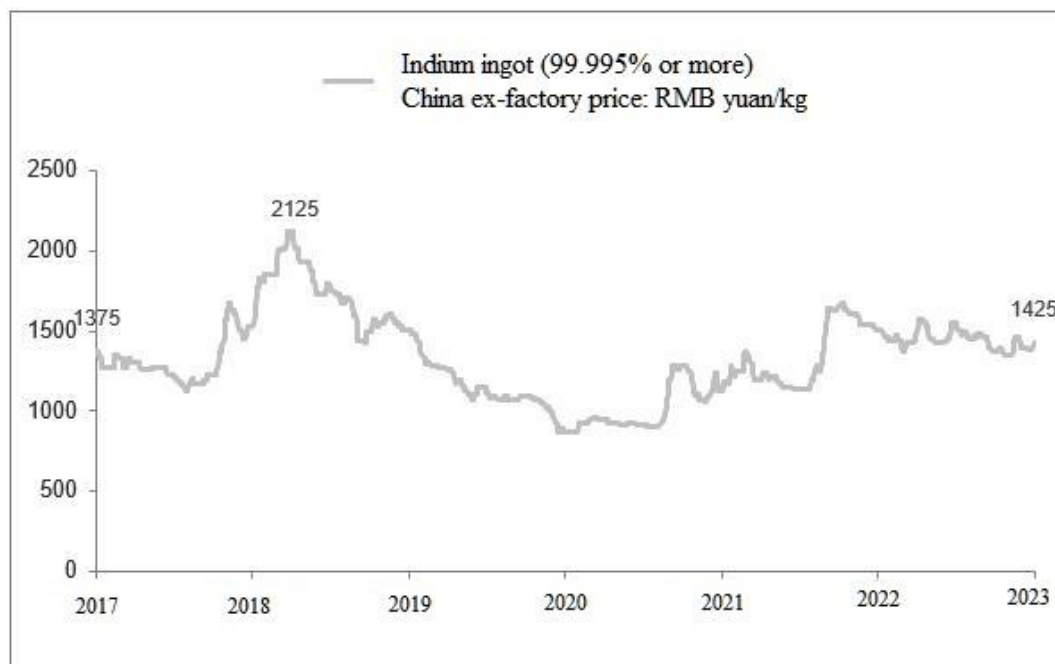


Figure 9. China's indium ingot price trend chart from 2017 to 2023<sup>8-10</sup>

Before the 2020 Spring Festival holiday, the successful auction of Pan Asia's indium inventory boosted market confidence to a certain extent. However, market demand is weak, industry pessimism is spreading, and prices are difficult to recover. From January to August 2020, the domestic indium price in China remained around RMB 900/kg. In September of the same year, the price of indium began to rise, but the market supply was large, and the holders were very motivated to ship. In addition, the market continued to grab market share due to tight funds, and the supplier had to lower the quotation again in December (Figure 9).

In 2021, due to the contraction of the supply side, a new round of downstream procurement, and the rise in electric board prices, market confidence was consolidated to a certain extent, leading to a slight increase in prices in March. But the good times did not last long, and prices fell again in April of the same year. In August, the domestic indium price in China gradually came out of the trough, and the growth rate accelerated in September. In the fourth quarter, the indium price remained at RMB 1,667/kg (Figure 9).

In 2022, the domestic indium price in China fell rapidly in the first quarter. In the second quarter, affected by speculative funds, the price of indium rose rapidly and then fell rapidly again. Entering the third quarter, due to continued weak demand, it stabilized slightly to RMB 1,528/kg in July and then fell back. In the fourth quarter, the price of indium remained bleak. In 2022, the average price of refined indium in China was RMB 1,495/kg, a year-on-year increase of 7.8% (Figure 9).

At present, China's indium production is in a state of oversupply, and the growth of domestic consumption is still insignificant compared with the potential for production growth. However, long-term large-scale export trade and abnormal trade behavior have always kept the country's indium market in a delicate balance. In addition, the pressure brought to the market by the 3,600 tons of inventory left by the Pan Asia Exchange still needs time to digest. Market fluctuations may be needed to provide opportunities for relief.

In the long run, against the background of steady growth in global indium consumption and accelerating domestic consumption, it is inevitable that prices will return reasonably from the low-cost area. But this takes time. Judging from the current situation, the indium product industry will still endure a period of low prices. But in terms of market sentiment, trading confidence will gradually recover in the next two years, and trading will also tend to be active, and it is an inevitable trend to push up indium prices overall.

The reason is that indium is considered a critical element worldwide due to its specific function in low-carbon technology and its vulnerability to supply disruption<sup>11</sup>. As the world is actively advocating low-carbon life, the price of indium products still has a lot of room to rise. The demand for In is expected to increase over the next several decades, with projections of up to 231 % by 2050 compared to 2018 production levels<sup>23</sup>.

### 5 Deposit type

As mentioned earlier, most rare dispersed elements, including indium, do not have independent primary deposits, at least for now. The reality is that most rare elements are by-products of other bulk minerals, namely, so-called associated, symbiotic or parasitic deposits. Mejías et al. (2023)<sup>11</sup> showed that the highest indium content has been commonly described in Cu-rich parts of polymetallic deposits related to magmatic-hydrothermal sources, in contrast with lower indium content in deposits formed at low temperatures and involving diagenetic processes. Sphalerite is the main In-bearing mineral phase incorporated indium through couple substitution, involving Cu, Ag, Ge, Ga, and Sn. Magmatic-hydrothermal sphalerite tends to be characterized by higher In, Cu, Sn, and Fe, and lower Ge contents and is associated with chalcopyrite, stannite, k esterite, cassiterite, and magnetite, which involve exsolution processes.

Based on the previous research data<sup>11, 22-34</sup>, especially the latest research results of Mejías et al.<sup>11</sup>, the genetic types of associated indium deposits known to humans are summarized in Table 2. The global spatial distribution of these associated indium deposits of different genetic types is shown in Figure 2 of this article.

**Table 2.** Genetic types and representative deposits of indium deposits around the world<sup>11, 22-34</sup>

Deposit type	Primary ore mineral	Main In-bearing minerals	Representative deposit
Skarn	Sn, Zn, Cu, Ag, Bi, As	sphalerite, chalcopyrite and andradite garnet	Dachang, Dulong, Yejiwei, and Qibaoshan in China
V(H)MS	Cu, Zn	sphalerite and chalcopyrite	María Teresa deposit in Peru, Gaiskoye deposit in Russia, Neves-Corvo in Portugal, and the Geco deposit in Canada
(Sn)PXV	Cu, Zn, Sn, Ag	Fe-rich sphalerite and stannite	Toyoha deposit in Japan; the Huari Huari, Potosi, and Bolivar mines in Bolivia
SEDEX		galena, sphalerite, chalcopyrite, and pyrite	Broken Hill in Australia; Dabaoshan mine in China
Epithermal vein	Zn, Pb, Cu, Au, Ag	gold, enargite, covellite, pyrite, sulphide, rhodonite, chalcopyrite and stannite	epithermal deposits in Argentina & Peru; Ayawilca in Peru; Ashio and Ikuno mines in Japan
Granite-related	Sn, Zn, Cu,	sphalerite, chalcopyrite, stannite, k�esterite,	Tigrinoe & Pravourmiiskoe in Russia; Isabel and Baal Gammon deposits in Australia; Cho Don in China; Colquiri in Bolivia
Porphyry Sn	Sn, Zn, Cu	sphalerite, stannite	Central Andean Sn belt from southern Peru through Bolivia to northwest Argentina; the Mount Pleasant deposit in Canada
Porphyry Cu	Cu, Co, Au, Re, Ag	chalcopyrite	The Bingham Canyon/Kennecott Copper mine, and the Santa Rita mine in USA
MVT	Pb, Zn	sphalerite, galena, pyrite, and marcasite	the Lisheen Zn-Pb deposit in Ireland
SSC	Cu	chalcocite, bornite, chalcopyrite, digenite,	the Waterloo mine in Australia
		djurleite, anilite, galena, and sphalerite	
IOCG	Cu, Au, Fe, Ag, Co,	pyrrhotite, pyrite, chalcopyrite, bornite,	the Copper Blow Project in NSW, Australia; the Chaparra IOCG, Peru
	Ni, Bi, Se, Te, U,	chalcocite, sakuraiite	
	REE, F, Ba, Mo		
MSCD	Cu, Pb, Zn, Ag	sphalerite, pyrite, Chalcopyrite, galena,	the Waterloo, Queensland, Australia

Note: V(H)MS - Volcanic-hosted massive sulphide; SEDEX - sedimentary exhalative mineral deposits; (Sn)PXV - (Sn) polymetallic xenothermal/epithermal veins; MVT - Mississippi valley-type Zn-Pb; SSC - Sediment-hosted stratiform Cu; IOCG - Iron-oxide copper gold; MSCD - Metamorphosed sandstone-shale copper deposits



It should be noted that among the many genetic types of the above-mentioned associated indium deposits, skarn, massive sulfide and similar deposit types are the most important associated deposit types of indium, accounting for 29.2% and 28% of the world's potential indium resources, respectively. The second is epithermal and sedimentary lead-zinc deposits, accounting for 19.9% and 18.0% of the world's indium resources, respectively.

Werner et al. (2017) counted 101 deposits<sup>34</sup>, and the total indium resources of these deposits included in the statistics were 76,183 metric tons.

The world's most representative skarn-type associated indium deposits include the Dachang tin deposit in Guangxi, and the Dulong tin-zinc polymetallic deposit in Yunnan, China; the Ayawilca deposit in Peru, the Tellerhauser and Pohla-Globenstein deposits in Germany, and the East Kemptville deposits in Canada.

The epithermal and polymetallic vein-type associated indium deposits mainly include the Toyoha, Ashio, Akenobe and Ikuno deposits in Japan; the Potosi and Bolivar deposits in Bolivia, etc.

VMS and SEDEX type associated indium deposits are represented by VMS deposits such as Kidd Creek, Geco/Manitouwadge and Heath Steele in Canada; Gaiskoye, Podolskoye and Sibaiskoye in Russia; and SEDEX deposits such as Broken Hill in Australia, Malku Khota in Bolivia, Rammelsberg in Germany, and Filizchay in Azerbaijan.

## 6 Discussion and conclusions

Rare dispersed metals, including indium, are extremely rare in the earth's crust and have long been ignored by humans. However, with the development of modern science and technology, they play an increasingly important role and have increasingly wide applications on this earth.

Although people can find substitutes for these rare metals, in many ways, the inherent physical and chemical properties of these natural rare metals determine that they cannot be completely and perfectly replaced.

Because of the important role of rare dispersed metals such as indium, its future market will be more and more optimistic, and its prospects will be infinitely bright. Of course, it is not ruled out that its market will fluctuate to a certain extent due to unpredictable international situations, complex relations between countries and other factors.

The extraction and beneficiation technology of indium ore must also be continuously updated and upgraded in order to recover large amounts of waste rock from ancient mines with special but high-grade indium occurrence, including huge stocks of tailings from related abandoned mines.

As indium products play an increasingly important role and position, its secondary recycling not only deserves further attention, but also needs to be strengthened. Obviously, secondary recycling is cheaper and more economical than developing mines.

As far as humans know, all indium deposits in the world are associated with certain bulk primary mineral products. In other words, indium is a trace parasitic mineral that appears in bulk non-ferrous metal deposits such as copper, lead and zinc.

In terms of genetic type, the potential of indium ore resources is huge. Almost all endogenous non-ferrous metal deposits have indium ore as an important byproduct. Among all indium-containing minerals, sphalerite is undoubtedly the most important and the one from which humans currently obtain the most indium.

In the near future, it is not ruled out that new genetic types of associated indium ore will be discovered, such as pure sedimentary indium deposits with higher grades formed after weathering, denudation and sedimentation of other primary associated indium ores. At the same time, it cannot be ruled out that the world's first primary independent indium deposit will be discovered under special geological settings.

In this complex and ever-changing society, everything is possible.



## 7 References

1. Beckman. April 25, 2024. Chemical Book. [https://www.chemicalbook.com/NewsInfo\\_62795.htm](https://www.chemicalbook.com/NewsInfo_62795.htm). Retrieved May 13, 2024 (in Chinese).
2. Asian Metal. <http://baike.asianmetal.cn/metal/in/application.shtml>. Retrieved May 16, 2024 (in Chinese).
3. <https://www.ebaiyin.com/baike/379.shtml>. Retrieved May 16, 2024 (in Chinese).
4. Rudnick RL & Gao S. 2014. 4.1 - Composition of the continental crust. Holland DH & Turekian KK (Eds.). Treatise on Geochemistry (Second Edition) [J]. Elsevier, pp. 1-51, DOI: <https://doi.org/10.1016/B978-0-08-095975-7.00301-6>.
5. <https://zh.wikipedia.org/zh-cn/%E9%93%9F>. Retrieved May 21, 2024 (in Chinese).
6. <https://zh.wikipedia.org/zh-cn/%E9%93%9F>. Retrieved May 21, 2024 (in Chinese).
7. [https://www.sohu.com/a/402484114\\_660942](https://www.sohu.com/a/402484114_660942). June 1, 2020. Retrieved May 23, 2024 (in Chinese).
8. China Economic Research Institute. September 1, 2023. 2023 China Indium Industry Market Research Report. [https://www.sohu.com/a/716820994\\_120928700](https://www.sohu.com/a/716820994_120928700). Retrieved June 1, 2024 (in Chinese).
9. Peng ZW. February 13, 2023. [https://www.sohu.com/a/438371240\\_120113054](https://www.sohu.com/a/438371240_120113054). Retrieved June 7, 2024 (in Chinese).
10. China Economic Information Network. December 15, 2020. [https://www.sohu.com/a/438371240\\_120113054](https://www.sohu.com/a/438371240_120113054). Retrieved June 7, 2024 (in Chinese).
11. Mejías O, Parbhakar-Fox A, Jackson L, Valenta R & Townley B. 2023. Indium in ore deposits and mine waste environments: Geochemistry, mineralogy, and opportunities for recovery. *Journal of Geochemical Exploration*, 255. <https://doi.org/10.1016/j.gexplo.2023.107312>.
12. Yin JZ, Yin HY, Chao YH & Shi HY. 2024d. Energy and tellurium deposits. *AIMS Geosciences*, 10 (1): 28-42. DOI: 10.3934/geosci.2024002.
13. Yin JZ & Shi HY. 2019b. Nano effect mineralization of rare elements-taking the Dashuigou tellurium deposit, Tibet Plateau, Southwest China as the example. *Academia Journal of Scientific Research*, 7 (11): 635-642. DOI: 10.15413/ajsr.2019.0902.
14. Yin JZ, Xiang SP, Chao YH, Yin YH & Shi HY. 2023a. Petrochemical eigenvalues and diagrams for the identification of metamorphic rocks' protolith, taking the host rocks of Dashuigou tellurium deposit in China as an example. *Acta Geochimica*, 42 (1): 103-124. DOI: 10.1007/s11631-022-00583-6.
15. Yin JZ, Xiang SP, Yin HY, Shi HY & Chao YH. 2023c. Origin of the Dashuigou independent tellurium deposit at the southeastern margin of Qinghai-Tibet plateau: based on the abundances of trace elements in the country rocks. *Advances in Geological and Geotechnical Engineering Research*, 5 (4): 41-55. DOI: <https://doi.org/10.30564/aggr.v5i4.5967>.
16. Yin JZ, Yin HY, Chao YH, Xiang SP & Shi HY. 2024a. Geology and geochemistry of the only independent tellurium deposit in the world. *Naturalis Scientias*, 1(1): 1-31. *Naturalis Scientias*. DOI: <https://doi.org/10.62252/NSS.2024.1001>.
17. Yin JZ, He DS, Yin YH, Shi HY & Xiang SP. 2022d. On ore from the Dashuigou Tellurium Deposit, Tibet Plateau, Southwest China. *European Journal of Applied Sciences*, 10 (6): 458-472. DOI: 10.14738/aivp.106.13599.
18. Yin JZ & Shi HY. 2020a. Mineralogy and Stable Isotopes of Tetradyomite from the Dashuigou Tellurium Deposit, Tibet Plateau, Southwest China. *Scientific Reports*, 10: 4634. DOI: 10.1038/s41598-020-61581-3. [www.nature.com/scientificreports](http://www.nature.com/scientificreports).
19. Yin JZ. 1996a. The metallogenic model and mineralizing mechanism of the Dashuigou independent tellurium deposit in Shimian County, Sichuan—the first and the only independent tellurium deposit in the world. *Acta Geoscientia Sinica*, special issue: 93-97.
20. Yin JZ, Chao YH, Yin HY, Shi HY & Xiang SP. 2024c. Origin of the Dashuigou independent tellurium deposit at Qinghai-Xizang Plateau: constraints from the light stable isotopes C, O, and H. *Acta Geochimica*, DOI: 10.1007/s11631-023-00665-z. <https://doi.org/10.1007/s11631-023-00665-z>.
21. USGS. Indium. U.S. Geological Survey, Mineral Commodity Summaries, January 2023. <https://pubs.usgs.gov/periodicals/mcs2023/mcs2023-indium.pdf>. Retrieved June 7, 2024.
22. China Economic Industry Research Institute. 2024. China Indium Mining Industry Development Monitoring and Investment Strategic Planning Report 2024-2030. Internal Publishing (in Chinese).
23. Hund K, La PD, Fabregas TP, Laing T & Drexhage J. 2023. Minerals for climate action: The mineral intensity of the clean energy transition.



24. Xu J & Li XF. 2018. Spatial and temporal distributions, metallogenic backgrounds and processes of indium deposits. *Acta Petrologica Sinica*, 34 (12): 3611-3626 (in Chinese with English abstract)
25. Werner TT, Mudd MG & Jowitt MS. 2017. The world's by-product and critical metal resources part III: A global assessment of indium. *Ore Geology Reviews*, 86: 939-956. <https://doi.org/10.1016/j.oregeorev.2017.01.015>.
26. Benites D, Torró L, Vallance J, Laurent O, Valverde PE, Kouzmanov K, Chelle-Michou C & Fontboté L. 2021. Distribution of indium, germanium, gallium and other minor and trace elements in polymetallic ores from a porphyry system: The Morococha district, Peru. *Ore Geology Reviews*, 136, 104236.
27. Andersen JC, Stickland RJ, Rollinson GK & Shail RK. 2016. Indium mineralisation in SW England: host parageneses and mineralogical relations. *Ore Geology Reviews*, 78, 213-238. DOI: 10.1016/J.OREGEOREV.2016.02.019.
28. Andersson P. 2020. Chinese assessments of “critical” and “strategic” raw materials: Concepts, categories, policies, and implications [J]. *The Extractive Industries and Society*, 7 (1): 127-137.
29. Schwarz-Schampera U & Herzig PM. 2013. Indium: Geology, mineralogy, and economics [M]. Springer Science & Business Media. DOI: 10.1007/978-3-662-05076-7.
30. Xu J, Cook NJ, Ciobanu CL, Li X, Kontonikas-Charos A, Gilbert S & Lv Y. 2021. Indium distribution in sphalerite from sulfide–oxide–silicate skarn assemblages: a case study of the Dulong Zn–Sn–In deposit, Southwest China[J]. *Mineralium Deposita*, 2021, 56: 307-324. DOI: 10.1007/s00126-020-00972-y.
31. Ye L, Cook NJ, Ciobanu CL, Liu YP, Zhang Q, Liu TG, Gao W, Yang YL & Danyushevskiy L. 2011. Trace and minor elements in sphalerite from base metal deposits in South China: A LA-ICPMS study [J]. *Ore Geology Reviews*, 39 (4): 188-217. DOI: 10.1016/j.oregeorev.2011.03.001.
32. Zhao Z, Hou L, Ding J, Zhang Q & Wu S. 2018. A genetic link between Late Cretaceous granitic magmatism and Sn mineralization in the southwestern South China Block: A case study of the Dulong Sn-dominant polymetallic deposit [J]. *Ore Geology Reviews*, 93: 268-289.
33. Schwarz-Schampera U and Herzig PM. 2002. Indium, Geology, Mineralogy, and Economics. Berlin, Heidelberg: Springer Science Business Media.
34. Werner TT, Mudd, MG & Jowitt MS. 2017. The world's by-product and critical metal resources part III: A global assessment of indium. *Ore Geology Reviews*, 86: 939-956. DOI: <https://doi.org/10.1016/j.oregeorev.2017.01.015>.

#### Data availability

The data that support the findings of this study is available from the author upon reasonable request.

#### Declaration of competing interest

The author declares that he has no known competing financial interests or personal relationships that could have appeared to influence the work reported in this paper.

#### Use of AI tools declaration

The author declares that he has not used Artificial Intelligence (AI) tools in the creation of this article.





## Original Article

## Temporal and spatial distribution and genesis of primary indium deposits around the world

JZ Yin<sup>1,2,3</sup>

### Abstract

Because rare dispersed elements including indium play an increasingly extensive and indispensable role in the field of modern high technology, the exploration, development and research of its resources are in full swing. The abundance of indium in the earth's crust is extremely low, and its original independent deposits have not been found so far. Indium is mainly parasitic in bulk non-ferrous metal deposits in the form of associated by-products. Because of its origin, the genetic types of indium deposits are as diverse as those non-ferrous metal deposits it parasitizes. The distribution of indium in geological time and earth space is uneven. The formation of indium ore deposit is closely related to tectonic-magmatic activity. It is the product of plate tectonic movement, continental rifts and mantle plumes or mantle hotspots in the interior of ancient continents. The emergence of indium ore deposit is inseparable from magmatic activity, especially granite magmatic activity. Ore-forming materials mainly come from the upper mantle and/or deep crust. Indium deposits formed under high temperature conditions have enrichment mechanisms. In addition to the enrichment factors of traditional metal deposits, the enrichment of nano-scale indium minerals through the nano effect is also a very important enrichment method. The indium deposits formed at the end of the differentiation and evolution of granite magma may not be enriched in one go, but is the result of multiple enrichments.

**Key words:** Rare metal indium; primary associated deposit; genetic type; global temporal and spatial distribution; genesis

---

**Affiliation Info:** <sup>1</sup> Wuhan Institute of Technology, Wuhan 430205, China; <sup>2</sup> College of Earth Sciences, Jilin University, Changchun 130061, China; <sup>3</sup> Orient Resources Ltd., Canada

**Article Info:** Received: 1 June 11, 2024 / Revised: 11 June 2024 / Accepted: 27 June 2024 / Published Online: 30 June 2024.  
www.naturalisscientias.com

**Authors' Contact Info:** Yin, JZ: jzyin7@jlu.edu.cn

**Citation:** Yin, JZ. 2024. Temporal and spatial distribution and genesis of primary indium deposits around the world. *Naturalis Scientias*, 1 (2): 167-180. DOI: <https://doi.org/10.62252/NSS.2024.1012>.

**Copyright** © 2024 by the authors. Published by *Naturalis Scientias*. This is an open access article under the Creative Commons Attribution-NonCommercial 4.0 International (CC BY-NC 4.0) License. (<https://creativecommons.org/licenses/by-nc/4.0/>).

**Corresponding Author** : Yin, JZ, PhD, PGeo, Professor; Email: jzyin7@jlu.edu.cn

## 1 Introduction

Indium is a rare dispersed element. Like most other dispersed elements, the general public knows very little about indium. After all, an element like indium, which is extremely low in abundance in the earth's crust, is not as closely related to people's daily lives as iron, aluminum and copper. To paraphrase a line from a poem by Bai Juyi, a great poet of the Tang Dynasty in China:

A maiden of the Yangs to womanhood just grown, In inner chambers bred, to the world was unknown.

The "maiden of the Yangs" here is the subject of this article, indium.

There is an old saying among the ancient Chinese: things are precious because they are rare. This summary is appropriate for rare dispersed elements such as indium. The progress of science and technology and the widespread application of indium in modern high-tech fields have greatly improved the status and price of rare dispersed metals such as indium that were previously unknown to people. After being developed and utilized, indium can also be described by an ancient Chinese proverb:

After ten years' hard study noticed by none, his fame fills the land once honors are won.

Indeed, today's indium and its related products have different applications in many fields, especially in the fields of high technology and military defense. Its unique physical and chemical properties allow it to play a great role in different industries.

Because of this, there has been a global boom in indium ore deposits prospecting, exploration, development and research.

In view of this, this article will analyze the origin of indium deposits based on summarizing the temporal and spatial distribution patterns of indium deposits around the world and exploring their ore-controlling factors, so as to contribute to finding more and better natural indium ore resources.

## 2 Types of primary indium deposit

As far as we know, most of the rare dispersed elements, including indium, such as thallium, germanium, selenium, tellurium and rhenium, do not have their own independent primary deposits, but exist as associated and/or trace components in bulk non-ferrous metal deposits such as copper, lead, zinc and tin. In other words, indium ore deposit is what this article calls a parasitic mineral.

Tellurium originally had a similar fate to all other rare dispersed elements, that is, it was produced in non-ferrous metal deposits such as copper in the form of associated or symbiotic trace components. However, this situation of tellurium was completely broken in the 1990s by the discovery and development of the Dashuigou independent tellurium deposit located on the southeastern edge of the Qinghai-Tibet Plateau<sup>1-7</sup>.

There is no doubt that the discovery of the only independent tellurium deposit in the world has not only broken the traditional geochemistry and mineral geology that rare dispersed elements cannot form independent deposits, but also brought great hope to find other independent deposits of rare dispersed elements.

But so far, no primary independent deposits of indium have been found. All indium deposits currently being explored and developed are associated and/or deposits. That is, indium, as an associated and/or symbiotic trace element, exists in traditional bulk deposits such as copper, lead, zinc, tin, gold and silver, and is extracted as a by-product for human use.

Therefore, the so-called genetic type of indium deposits is actually the genetic type of deposits such as copper, lead, zinc, tin, gold and silver that people are more familiar with.

Based on the research results of predecessors and the author's personal research and development experience, the genetic types of primary associated indium deposits are briefly summarized in Table 1<sup>8-21</sup>. As for the global distribution of these different genetic types of indium deposits, please see Figure 1.

As can be seen from Figure 1, like most other minerals, the distribution of indium ore deposits in the world is seriously uneven, but concentrated in certain areas of the continental plate. Of course, these specific areas must be areas with superior metallogenic geological settings and conducive to the production of such minerals. According to the current calculation results, the world's associated indium deposits are mainly concentrated in a few countries

such as China, Peru, the United States, Canada and Russia. Among them, the indium reserves of the first three countries account for about 72.0%, 3.3% and .5% of the global total respectively<sup>22-23</sup>.

**Table 1.** Genetic types and representative deposits of associated indium deposits around the world<sup>8-21</sup>

Deposit type	Primary ore mineral	Main In-bearing minerals	Representative deposit
Skarn	Sn, Zn, Cu, Ag, Bi, As	sphalerite, chalcopyrite and andradite garnet	Dachang, Dulong, Yejiwei, and Qibaoshan in China
V(H)MS	Cu, Zn	sphalerite and chalcopyrite	María Teresa deposit in Peru, Gaiskoye deposit in Russia, Neves-Corvo in Portugal, and the Geco deposit in Canada
(Sn)PXV	Cu, Zn, Sn, Ag	Fe-rich sphalerite and stannite	Toyoha deposit in Japan; the Huari Huari, Potosi, and Bolivar mines in Bolivia
SEDEX		galena, sphalerite, chalcopyrite, and pyrite	Broken Hill in Australia; Dabaoshan mine in China
Epithermal vein	Zn, Pb, Cu, Au, Ag	gold, enargite, covellite, pyrite, sulphide, rhodonite, chalcopyrite and stannite	epithermal deposits in Argentina & Peru; Ayawilca in Peru; Ashio and Ikuno mines in Japan
Granite-related	Sn, Zn, Cu,	sphalerite, chalcopyrite, stannite, k�esterite,	Tigrinoe & Pravourmiiskoe in Russia; Isabel and Baal Gammon deposits in Australia; Cho Don in China; Colquiri in Bolivia
Porphyry Sn	Sn, Zn, Cu	sphalerite, stannite	Central Andean Sn belt from southern Peru through Bolivia to northwest Argentina; the Mount Pleasant deposit in Canada
Porphyry Cu	Cu, Co, Au, Re, Ag	chalcopyrite	The Bingham Canyon/Kennecott Copper mine, and the Santa Rita mine in USA
MVT	Pb, Zn	sphalerite, galena, pyrite, and marcasite	the Lisheen Zn-Pb deposit in Ireland
SSC	Cu	chalcocite, bornite, chalcopyrite, digenite, djurleite, anilite, galena, and sphalerite	the Waterloo mine in Australia
IOCG	Cu, Au, Fe, Ag, Co,	pyrrhotite, pyrite, chalcopyrite, bornite,	the Copper Blow Project in NSW, Australia; the
	Ni, Bi, Se, Te, U, REE, F, Ba, Mo	chalcocite, sakuraiite	Chaparra IOCG, Peru
MSCD	Cu, Pb, Zn, Ag	sphalerite, pyrite, Chalcopyrite, galena,	the Waterloo, Queensland, Australia

Note: V(H)MS - Volcanic-hosted massive sulphide; SEDEX - sedimentary exhalative mineral deposits; (Sn)PXV - (Sn) polymetallic xenothermal/epithermal veins; MVT - Mississippi valley-type Zn-Pb; SSC - Sediment-hosted stratiform Cu; IOCG - Iron-oxide copper gold; MSCD - Metamorphosed sandstone-shale copper deposits

Europe also widely develops hydrothermal vein-type associated indium deposits related to granite, such as the South Crofty area in southwest England (1 t) and the West Shropshire ore field (1 t), the Freiberg area in Germany (45 t), the Langban deposit in Sweden (1 t), and the Wiborg batholith in Finland (Werner et al., 2017)<sup>12</sup>. However, compared with similar indium deposits in other countries such as China, the resources of the above-mentioned European indium deposits are relatively much less.

The uneven distribution of different minerals on the earth's surface depends on the different geochemical properties of different elements on the one hand, and on the other hand, it is related to the earth's differentiation and evolution process and later tectonic-magmatic activities.

### 3 Metallogenic environment

A deep understanding of the formation environment of a mineral deposit is an important basis for exploring its origin and is also the only way to find more similar mineral deposits.



**Figure 1.** Map of the world's typical indium deposits<sup>8-9</sup>

Note: For the meaning of the abbreviations in the figure, please refer to the footnotes of Table 1

### 3.1 Geotectonic

Regarding the tectonic location of primary indium deposits, Schwarz-Schampera & Herzig (2002)<sup>24</sup> believed that the formation of indium deposits is closely related to plate subduction, collision and orogenic activities. Therefore, they are mainly distributed at the edges of active oceanic or continental plates, and near orogenic belts where geothermal gradients change sharply due to tectonic-magmatic activities.

This is true. An indisputable fact is that one of the most important indium mineral belts in the world is right next to the edge of the subduction zone on the west side of the Pacific plate (Figure 1)<sup>8-9</sup>. This indium mineral belt includes the Toyoha (4651 t), Ashio (1,240 t), Ikuno (1,094 t) and Akenobe (875 t) indium deposits in Japan, and the Ulsan indium deposit (90 t) in South Korea.

Another indium mineral belt is centered in Bolivia and Peru on the eastern edge of the South American plate and extends northward to the western edge of the North American plate (Figure 1). As far as we know, the indium resources in this indium mineral belt are mainly concentrated in Bolivia, accounting for nearly 20.0% of the global total<sup>12</sup>. The indium mineral genetic types are also very diverse, including epithermal silver-tin polymetallic deposits such as Huari Huaru (5,601 t), Potosi (4,030 t) and Bolivia (2,311 t); and SEDEX-type indium-bearing lead-zinc deposits such as Malku Khota (2,431 t).

The third indium belt is centered in the Alpine orogenic belt in central Europe and extends to western Russia. The countries and indium deposits covered include Neves Corvo (3,480 t) in Portugal, Tellerhäuser (2,286 t) and Erzberg (1,470 t) in Germany, and VMS-type copper-zinc-(lead) deposits such as Gaiskoye, Podolskoye (485 t) and Sibaiskoye (1,000 t) in Russia. The Gaiskoye associated indium deposit is the largest indium deposit known in the world thus far, about 9,120 t) (Figure 1).

Other important indium deposits in other parts of the world include Broken Hill (2,659 t) in Australia, Mount Pleasant (1,246 t) and Kidd Creek (1,900 t) in Canada, and Kingman (1,109 t) in the United States.

Large associated indium deposits in ancient continents far from the plate subduction zones are most likely related to the activity of mantle plumes and/or mantle hotspots. For indium-bearing massive sulfide deposits in volcanic rocks

and exhalative sedimentary rocks, the favorable tectonic background is the back-arc environment and rift environment, and the favorable surrounding rocks are felsic rather than mafic rocks.

Relevant statistics show that associated indium deposits in China are highly concentrated in the eastern section of the Central Asian Orogenic Belt and South China<sup>21</sup>. Therefore, at present and for a long time before, the exploration, development and research of indium deposits in China are mainly concentrated in the southwestern margin of the Yangtze Platform in the country.

Tu et al. (2004) concluded that China's indium-rich deposits are mainly located on the edge of ancient continents. Among them, the south-southwestern margin of the Yangtze Plate is the country's most important distribution area of large and super-large indium-rich deposits<sup>25</sup>. The area includes the Dachang tin polymetallic ore field located in the southwestern margin of the Jiangnan Ancient Continent and the northern fault depression basin of the Hercynian-Indosinian passive continental margin rift basin, as well as the western end of the South China folded belt, the Yangtze Massif, and the Ailao Mountains. The Dulong tin polymetallic deposit is located at the intersection of three major structural units in the folded belt. On the northern edge of the North China Plate, there are also some large-scale indium-tin-rich polymetallic deposits distributed, such as the Meng'en Tolgoi (>500 t, Zhang et al., 2006)<sup>26</sup> in Inner Mongolia and Oi deposit (>768 t, Ishihara et al., 2008)<sup>27</sup>.

Obviously, the local concentrated development of indium deposits is also affected and controlled by the special structural geological environment at the edge of the ancient continent (Zhang et al., 2003; Cheng, 2013)<sup>28-29</sup>.

Other areas and deposits containing indium in China include: the Cambrian indium-bearing gold deposit in the western Qinling Mountains (Liu et al., 1998)<sup>30</sup>; the Chahe tin deposit in Sichuan (Guo et al., 2006)<sup>31</sup>; the indium-bearing deposits in the Bangong Lake-Nujiang River metallogenic belt in Tibet, such as the Lawu skarn copper-zinc deposit (Zhao et al., 2010)<sup>32</sup>; the high-sulfur gold-copper deposit in Zijinshan, Fujian, which contains roquesite (CuInS<sub>2</sub>) (Wang et al., 2014)<sup>33</sup>; and the copper-tin-indium deposit in the Saishitang-Rilonggou ore field in Qinghai (Liu et al., 2016)<sup>34</sup>. Indium minerals or indium mineralization have also been discovered in deposits such as Qibaoshan (Liu, 2017)<sup>35</sup>, Xianghualing (Liu et al., 2017)<sup>36</sup> and Yejiwei (Liu et al., 2018)<sup>37</sup> in Hunan Province.

An interesting phenomenon is that the world's important indium metallogenic belts coincide with the world's main tin mineralization belts. For this reason, Chen & Zhao (2021) concluded that<sup>28</sup>, the important source of indium is tin polymetallic deposits associated with granite. If this statistic is representative enough, then the tin deposit itself is one of the important prospecting signs of associated indium ores.

Werner et al. (2017) believed that<sup>12</sup>, Australia, Russia, Canada and other countries have a large number of large and super-large lead-zinc deposits. It is speculated that the indium resources in these countries have considerable prospects.

### 3.2 Ore-forming rock

Schwarz-Schampera & Herzig (2002) concluded that the hydrothermal system with the highest indium content usually appears in the back-arc rift environment and related island arcs, and is closely related to the developed bimodal volcanic activity and volatile-rich magma<sup>20</sup>. Partial melting and assimilation of the ancient crust may play an important role in the enrichment of incompatible elements indium in high-fraction arc magma.

Chen & Zhao (2021) concluded through research that an important source of indium is tin polymetallic deposits related to granitic magma<sup>38</sup>. During the evolution of the magma-hydrothermal system, tin and indium are enriched simultaneously. During this period, if the main carrier minerals of indium, such as biotite and hornblende, crystallize and separate, the mineralization potential of indium will be greatly weakened. After entering the ore-forming fluid, indium is mainly transported in the form of chloride, fluoride and hydroxide. Fluid temperature, pH, and the type and concentration of metal ligands are important factors controlling indium migration and precipitation. When indium precipitates from the fluid, the four-fold coordinated In<sup>3+</sup> is more similar to the four-fold coordinated metal ions in base metal sulfides such as sphalerite, chalcopyrite and tetrahedrite, causing a large amount of indium to enter the sulfide by isomorphic substitution and separate from tin. The precipitated indium-containing minerals may be reactivated, migrated and diffused in the later geological process, leading to the re-enrichment of indium. The enrichment of indium is closely related to tin, most likely due to the similar geochemical properties of indium and tin. In the supergene environment, indium and tin are retained in clay-rich sedimentary rocks undergoing chemical weathering due to reduced activity. This sedimentary rock will form a large number of mica minerals after

metamorphism. The decomposition of biotite, a common carrier of indium and tin, under high temperature conditions may be the fundamental reason for the simultaneous enrichment of indium and tin in the deposit.

However, indium in some newly discovered tin-poor magmatic hydrothermal deposits is also abnormally enriched.

#### 4 Metallogenic era

According to statistics from Werner et al. (2017)<sup>12</sup>, China's indium resources account for 18.2% of the world's total. These are mainly associated indium deposits of skarn-type tin polymetallic deposits, such as Dachang (8,775 t) in Guangxi, Dulong (5,124 t) and Gejiu (>4,000 t) in Yunnan, which were formed in the Late Cretaceous. Zheng et al. (2023) found that 85% of the associated indium deposits were formed in the Mesozoic, and the number of deposits before the Mesozoic was relatively small<sup>21</sup>.

Xu & Li (2018) selected 34 relatively typical indium-rich deposits from 101 publicly published in the world for relevant statistical analysis and research<sup>9</sup>. The total indium resources of these 34 indium deposits accounted for more than 95% of the known global indium resources at that time. In order to reflect the relationship between the mineralization of indium and geological evolution in different geological periods, Figure 2 shows the corresponding relationship between the genetic type, formation age and resource volume of these 34 indium deposits. As can be seen from Figure 2, the global large-scale indium mineralization is concentrated in the three geological periods of the Neogene, Cretaceous and Devonian. The corresponding indium ore genetic types of these three important indium mineralization periods are epithermal-tin polymetallic vein type, skarn type and VMS type.

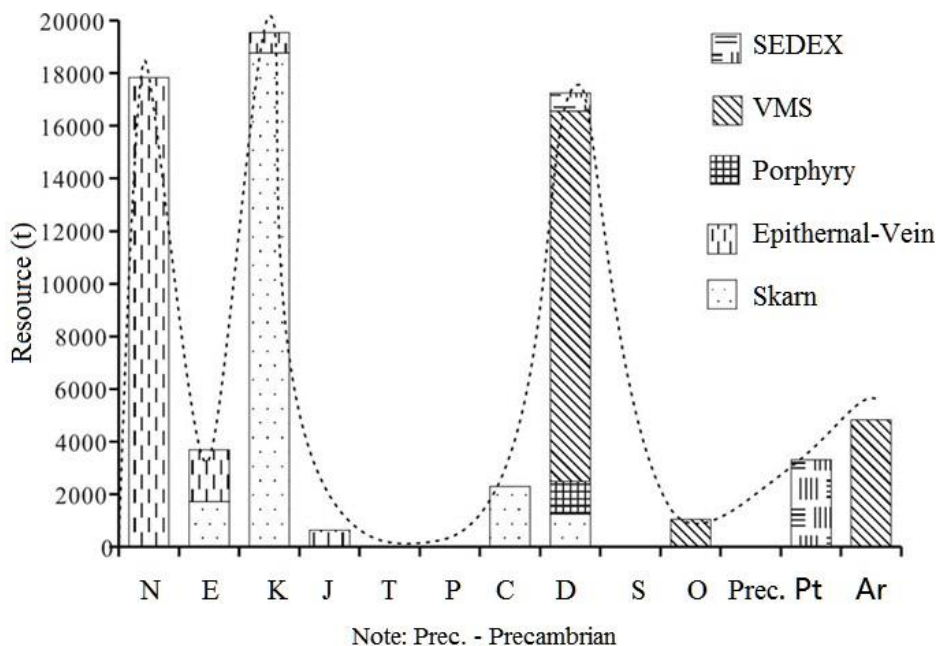


**Figure 2.** Distribution diagram of indium ore resources in different geological periods around the world<sup>9</sup>

#### 5 Deposit geology

All the currently known associated indium deposits in the world are produced in igneous rocks, especially granite intrusive and/or its surrounding rock contact zones. The formation of these indium deposits has a close genetic and direct spatial connection with tectonic-magmatic activities.

As for the carrier minerals of indium, no matter how the indium deposits are formed, that is, no matter what their genetic type is, indium is without exception mainly found in sphalerite<sup>21</sup>. This is already a consensus in the global geological community.

At present, more than 20 independent indium minerals have been identified in the world, including native indium (In), roquesite (CuInS<sub>2</sub>), sakuraiite ((Cu,Zn,Fe)<sub>3</sub>(InSn)S<sub>4</sub>), dzhalindite/jalindite (In(OH)<sub>3</sub>), indite (FeIn<sub>2</sub>S<sub>4</sub>), dzhalindite (In(OH)<sub>3</sub>), indite (FeIn<sub>2</sub>S<sub>4</sub>), ishiharaitite (Cu,G,Fe,In,Zn)S, abramovit (Pb<sub>2</sub>SnInBiS<sub>7</sub>), ramdohrite (Pb<sub>5,9</sub>Fe<sub>0,1</sub>Mn<sub>0,1</sub>In<sub>0,1</sub>Cd<sub>0,2</sub>Ag<sub>2,8</sub>Sb<sub>10,8</sub>S<sub>24</sub>), znamenskyite (Pb<sub>4</sub>In<sub>2</sub>Bi<sub>4</sub>S<sub>13</sub>), cadmoindite (CdIn<sub>2</sub>S<sub>4</sub>), laforetite (AgInS<sub>4</sub>), damiaoite (PtIn<sub>2</sub>), yixunite (Pt<sub>3</sub>In), abramovite (Pb<sub>2</sub>SnInBiS<sub>7</sub>), yanomamite (InAsO<sub>4</sub>·2H<sub>2</sub>O), polywurtzite ((Cu,Fe,Zn,Ag)<sub>3</sub>(Sn,In)S<sub>4</sub>) or ((Cu, Zn, Fe, In, Sn)S), and three unnamed minerals ZnCdIn<sub>2</sub>S<sub>7</sub>, ZnCdIn<sub>2</sub>S<sub>5</sub> and CdInS<sub>4</sub>. Ishiharaitite was first discovered by Márquez-Zavalía in the Capillitas deposit in northwestern Argentina in 2014 and named after Japanese scholar Dr. Shunso Ishihara.

China has currently discovered five of them, among which roquesite is the most common and widely distributed indium independent mineral in China's associated indium deposits. The remaining indium independent minerals, such as native indium and dzhalindite/jalindite, only appear in small quantities in specific associated indium deposits<sup>21</sup>.

Tables 2 and 3 list the simple compounds of indium and the most widely distributed indium-containing minerals, respectively.

**Table 2.** Simple compounds of indium<sup>39</sup>

Compound	Mineral name	Chemical formula
Nitride	indium nitride	InN
Sulfide	indium sulphide	InS
	diindium trisulphide	In <sub>2</sub> S <sub>3</sub>
Selenide	indium selenide	InSe
	diindium triselenide	In <sub>2</sub> Se <sub>3</sub>
Telluride	indium telluride	InTe
	diindium tritelluride	In <sub>2</sub> Te <sub>3</sub>
Hydride	indium hydride	InH
Fluoride	indium trifluoride trihydrate	InF <sub>3</sub> ·3H <sub>2</sub> O
	indium fluoride	InF
	indium trifluoride	InF <sub>3</sub>
	indium trifluoride nonahydrate	InF <sub>3</sub> ·9H <sub>2</sub> O
Chloride	indium chloride	InCl
	indium dichloride	InCl <sub>2</sub>
	indium trichloride	InCl <sub>3</sub>
Bromide	indium bromide	InBr
	indium dibromide	InBr <sub>2</sub>
	indium tribromide	InBr <sub>3</sub>
Iodide	indium iodide	InI
	indium triiodide	InI <sub>3</sub>
	diindium tetraiodide	In <sub>2</sub> I <sub>4</sub>
Oxide	indium oxide	InO
	diindium trioxide	In <sub>2</sub> O <sub>3</sub>

**Table 3.** Most widespread minerals containing indium<sup>39</sup>

Name	Formula	Crystal System	Mindat Localities
Roquesite	CuInS <sub>2</sub>	Tetragonal	62
Ramdohrite	Pb <sub>5.9</sub> Fe <sub>0.1</sub> Mn <sub>0.1</sub> In <sub>0.1</sub> Cd <sub>0.2</sub> Ag <sub>2.8</sub> Sb <sub>10.8</sub> S <sub>24</sub>	Monoclinic	43
Dzhalindite	In(OH) <sub>3</sub>	Isometric	18
Sakuraiite	(Cu,Zn,Fe) <sub>3</sub> (In,Sn)S <sub>4</sub>	Isometric	15
Indium	In	Tetragonal	10
Laforêtite	AgInS <sub>2</sub>	Tetragonal	3
Cadmoindite	CdIn <sub>2</sub> S <sub>4</sub>	Isometric	3
Indite	FeIn <sub>2</sub> S <sub>4</sub>	Isometric	2
Yanomamite	InAsO <sub>4</sub> ·2H <sub>2</sub> O	Orthorhombic	2
Damiaosite	PtIn <sub>2</sub>	Isometric	2

Note: This list of minerals containing indium is built from the mindat.org locality database.

This is based on the number of localities entered for mineral species and is therefore slanted

towards minerals interesting to collectors with less coverage of common

rock-forming-minerals so it does not give an undistorted distribution of Indium mineral species.

It is more useful when comparing rare species rather than common species.

As the third largest cassiterite sulfide deposit in China, the Dulong tin-zinc polymetallic deposit in Yunnan China has been proposed by some researchers as a composite control of granite, structure and stratigraphy<sup>40-42</sup>. The late Yanshanian granitic magmatism is the provider of the main ore-forming materials and ore-forming energy, and is the key to the formation of the deposit. The structure and stratigraphy provide favorable channels, space and physical-chemical environment for the migration, enrichment and precipitation of ore-forming materials. The deposit is of magmatic hydrothermal origin.

As for the large-scale polymetallic massive sulfide deposits such as Gejiu and Bainiuchang in eastern Yunnan, China, many early researchers believed that they were typical magmatic hydrothermal deposits. Recently, some researchers have found through systematic studies of sulfide minerals in these deposits that these so-called typical magmatic hydrothermal deposits are actually massive sulfide deposits of submarine jet deposition, because oolitic, spherical and strawberry-like textures, as well as banded and lamellar structures were found in these ore bodies<sup>40</sup>.

Guo et al. (2006)<sup>31</sup> found through research that the indium content in the Chahe tin polymetallic ore area in Sichuan, China is very high, up to  $186.5 \times 10^{-6}$ . In addition, through the correlation analysis of indium and other ore-forming elements, it was found that indium in the area has a significant positive correlation with Zn, Cu, Fe, Cd, Sn, and Ga. It is speculated that indium may exist in the sulfides and/or (tin) oxides of these metals. Further electron probe analysis found that indium in the study area is mainly present in sphalerite, with a maximum content of  $500 \times 10^{-6}$ .

Zhao et al. (2010)<sup>32</sup> found that the average grade of indium in 18 deposits (showings) located in the Bangong Lake-Nujiang River metallogenic belt and adjacent areas in Tibet, China, meets the requirements of associated industrial grade. All samples with high indium content were collected from skarn-type deposits with a belt-like distribution. The indium minerals are mainly dzhalindite and native indium. The Lawu polymetallic deposit in Dangxiang County in the area, which is currently being mined, has an average indium content of  $45.44 \times 10^{-6}$  and a maximum of  $166 \times 10^{-6}$ .

Wang et al. (2014) discovered the relatively rare indium-independent mineral roquesite for the first time in China when studying the mineral composition of deep ore in the Zijinshan copper-gold deposit in Fujian, China<sup>33</sup>. Roquesite is usually found in medium- and high-temperature hydrothermal deposits. High-temperature minerals such as kiddcreekite, hemusite, colusite, mawsonite, stannite and molybdenite appear in the copper ore bodies in the southeastern section of the Zijinshan copper-gold deposit, indicating that the mineralization temperature in the deep part of the Zijinshan deposit is relatively high, and the contents of In, Sn, Pb, Zn, Mo and W in the ore-forming fluid are also relatively high.

## 6 Mineralization mechanism

Plate tectonic movement and orogenic movement are the most important driving forces for the formation of associated indium deposits and their host deposits.

These powerful forces not only produce strong tectonic-magmatic activities, but also drive the activation, enrichment and migration of various metal minerals and trace elements including various independent indium minerals. These ore-forming materials, which mainly come from the upper mantle and deep crust, not only gradually enrich in the process of magma differentiation, but also gradually reach a certain concentration with the increase of active liquid components. After finally rising to a certain part of the upper crust, due to changes in various physical and chemical conditions such as temperature and pressure, pH, salinity, sulfur fugacity and oxygen fugacity, they emplace in suitable structure and the contact zone between the intrusive and the sedimentary rock to form deposits of different genetic types.

As a copper-loving (sulfur-loving) element, indium is usually distributed in the mantle and crust in the form of  $\text{In}^{3+}$  (Smith et al., 1978)<sup>43</sup>. In the absence of sulfides during crustal differentiation, indium can show the characteristics of lithophile elements (Jenner and O'Neill, 2012)<sup>44</sup>. In the process of magma fractionation, indium is an incompatible element. Therefore, in the late stage of magma crystallization fractionation, most of the indium is retained in the solution. At this point, the fractionation evolution of indium is likely to be similar to that of tin, and it is highly volatile and can migrate in high-temperature gases such as HCl and HF at up to 940 °C (Kovalenker et al., 1993)<sup>45</sup>.

The content of indium in the mantle is about  $18 \pm 3 \times 10^{-9}$  (Witt-Eickschen et al., 2009)<sup>46</sup>,  $0.08 \times 10^{-6}$  in meteorites (Anders & Grevesse, 1989)<sup>47</sup>,  $0.05 \times 10^{-6}$  in the continental crust and  $0.072 \times 10^{-6}$  in the oceanic crust (Taylor & McLennan, 1985)<sup>48</sup>.

Liu (1984) pointed out that in most cases, high temperature conditions are conducive to the enrichment of indium<sup>49</sup>. The research results of most indium deposits also reveal that they are usually formed under high temperature conditions<sup>50-54</sup>. The increase in temperature may be conducive to improving the binding ability of indium with complex ions, and reach the maximum at 300~350 °C<sup>55</sup>.

Statistics show that the indium content in tin-rich sulfide deposits is relatively high, averaging above  $80 \times 10^{-6}$ . It shows that tin plays an important role in the enrichment of indium<sup>25,28,56</sup>. Zhang et al. (2007) pointed out by comparing China's indium-rich and indium-poor lead-zinc deposits that tin and indium are co-enriched and migrated in the ore-forming fluid until they are separated in the mineralization precipitation process<sup>57</sup>. Liu et al. (1984) found that a common feature of indium-rich minerals in crystal structure is that they all have a tetrahedral structure<sup>49</sup>. It is inferred that the tin-containing hydrothermal system is conducive to the enrichment and migration of indium, so indium can reach a higher concentration in the ore-forming solution. However, in the final precipitation process, after indium and tin parted ways, a large amount of indium entered into sphalerite with hexahedral coordination (Tu Guangchi, 2004)<sup>25</sup>.

Although existing statistics show that the vast majority of indium-rich ( $\text{In} > 100 \times 10^{-6}$ ) deposits in the world are closely related to tin-rich magmatic hydrothermal systems, while the grade and reserves of indium in tin-poor deposits are relatively low<sup>9</sup>. And some researchers have concluded that the tin-rich ore-forming fluid is the main controlling factor for the abnormal enrichment of indium metal in the deposit and its high grade and high reserves. But this does not mean that tin mineralization contributes to the mineralization enrichment of indium, at least the author of this article holds such a view. It can only be said that the mineralization geological conditions and physical and chemical conditions of indium and tin happen to be extremely close or very similar. On this point, more representative statistics and relevant in-depth research can draw more convincing conclusions.

The tin-rich indium deposits are mainly granite-related skarn type, shallow low-temperature hydrothermal type and hydrothermal vein type<sup>9</sup>. Representative deposits include the tin-rich copper-zinc deposits in Dulong, Dachang, Gejiu in China; Japan, Bolivia, Mount Pleasant in Canada; the Iberian pyrite belt in Portugal, and related deposits in the Russian Far East.

The indium deposits without tin are mainly VMS and SEDEX Cu-Pb-Zn deposits, but the grade and reserves of indium in these deposits are relatively low. Representative deposits include the Langban exhalative sedimentary Fe-Mn (Pb-Zn-Cu) deposit in Bergalagen, Sweden, and some base metal massive sulfide deposits in Siberia, Russia<sup>9</sup>.

Indium is an incompatible element in the process of magma fractionation. Therefore, in the late stage of magma crystallization fractionation, most of the indium tends to remain in the melt, and its fractionation evolution may be similar to that of tin (Kovalenker et al., 1993)<sup>45</sup>. Therefore, indium mineralization is often closely related to highly differentiated granites.

## 7 Discussion

Relevant studies have shown (Chen et al., 2008; Datta et al., 2009) that as a highly volatile sulfur-loving element, indium shows moderate to high incompatibility in mantle melt<sup>58-59</sup>. Due to its volatility, indium can be combined with sulfur in the form of gas and is widely used in nanomaterials.

Considering that the above-mentioned indium deposits around the world are mostly, if not all, formed in high-temperature environments, indium can be combined with sulfur in the form of gas to reach the nanometer level. It is certain that, like other rare dispersed elements, the enrichment of indium is closely related to the nano effect, which is the nano effect enrichment and mineralization mechanism proposed by the authors of this article.

The formation of indium deposits is inseparable from tectonic-magmatic activities. For example, a large number of indium-rich tin polymetallic deposits related to young volcanic activities in Bolivia show the affinity of indium with volcanic-magmatic systems (Sugaki et al., 1983)<sup>60</sup>. In epithermal mineralization systems, the close relationship between indium and magmatic activity is more obvious, such as the Pinguino indium deposit related to Jurassic magmatic activity in the Deseado Massif area of Argentina (Jovic et al., 2011a, 2011b, 2011c)<sup>61-63</sup>. The close connection between granite intrusions and indium mineralization further shows that the formation of indium ore deposits cannot be separated from the help of igneous rocks. In other words, tectonic-magmatic activity is one of the most important factors in the formation of indium deposits. The relevant evidence is as follows:

Valkama et al. (2016a) confirmed that indium-containing polymetallic veins were developed in the rapakivik granite developed in the Sarvixviken area of Finland<sup>64</sup>. The world's second polymetallic skarn mineralization system (Sn, W, Mo, Be, In) was discovered in the Pitkaranta region of Russia, which is related to the rapakivi granites in the region. Shimizu & Morishita (2012) studied the Toyoha deposit in Japan and concluded that indium mineralization is closely related to porphyry dykes and/or stocks formed in the late magmatic period<sup>54</sup>.

Zhang et al. (2003) proposed that the Meng'en Tolgoi, Jubankeng, Gejiu and other deposits in China are closely related to magmatic activity, and indium may be mainly derived from magmatic activity<sup>28</sup>. The indium content of muscovite plagioclase granite in the Meng'en Tolgoi deposit in China is  $1 \times 10^{-6} \sim 7 \times 10^{-6}$ , which is 10~70 times the Clark value (Li et al., 2007)<sup>65</sup>. The high indium content ( $>0.14 \times 10^{-6}$ ) in the east and west dykes in the Dachang mining area in Guangxi China also indicates that the indium and tin in Dachang originated from the magmatic source related to granite<sup>66</sup>. Skarn-type indium mineralization also confirms its genetic relationship with magmatic activity, the most typical of which is Dachang mine in Guangxi, and Dulong mine in Yunnan, China (Werner et al., 2017)<sup>12</sup>.

There are also a large number of examples of indium mineralization related to magmatic rocks in other countries, such as the Vaulry and Charrier mines in France (Cantinolle et al., 1985)<sup>67</sup>, the Mangabeira mine in central Brazil (Moura et al., 2014)<sup>68</sup>, and the Mount Pleasant mine in Canada (Sinclair et al., 2006)<sup>69</sup>.

These deposits are almost all related to A-type or S-type granites. A-type and S-type granites are usually closely related to metal mineralization such as tungsten, tin, molybdenum, and rare metals, and often show the characteristics of highly differentiated granites (Wu et al., 2017)<sup>70</sup>. Except for the Late Cretaceous and a small amount of Late Jurassic in China, the formation age of granites in other countries is mostly concentrated in the Proterozoic and Carboniferous-Devonian<sup>9</sup>. Of course, not all S-type and A-type granites are accompanied by indium mineralization.

## 8 Conclusions



Indium mineralization, which mainly exists as an associated or paragenetic component of traditional bulk nonferrous metal mineral deposits, has a variety of genetic types. Indium deposits basically have the genetic types of other endogenous metal minerals.

The formation of indium deposits is inseparable from tectonic-magmatic activities. Especially plate tectonic movement, orogeny, continental rifting, mantle plume and mantle hotspot activities.

Large-scale tectonic-magmatic activities are the huge driving force for the formation of indium deposits. Especially the granitic magmatic activities in the mantle source and/or deep crust not only provide metallogenic power, but also provide the source of ore-forming materials.

Considering the extremely low abundance of indium in the earth's crust, the enrichment of indium ore-forming materials may not be completed in one go, but is jointly promoted by different geological processes and other processes including the nano effect; that is, the result of multiple enrichments. Indium mineralization, which mainly originates from the upper mantle and occurs under high temperature conditions, has excellent natural conditions for the enrichment of nano-scale ore-forming materials.

With the continuous deepening of research, it is not ruled out that new genetic types of associated indium deposits will be discovered in the future, such as sedimentary rock type, metamorphosed sedimentary rock type, etc. It is also not ruled out that the world's first primary independent indium deposit will be discovered under special geological background somewhere on the earth.

## 9 References

1. Yin JZ & Shi HY. 2019b. Nano effect mineralization of rare elements-taking the Dashuigou tellurium deposit, Tibet Plateau, Southwest China as the example. *Academia Journal of Scientific Research*, 7 (11): 635-642. DOI: 10.15413/ajsr.2019.0902.
2. Yin JZ & Shi HY. 2020a. Mineralogy and Stable Isotopes of Tetradyomite from the Dashuigou Tellurium Deposit, Tibet Plateau, Southwest China. *Scientific Reports*, 10: 4634. DOI: 10.1038/s41598-020-61581-3. [www.nature.com/scientificreports](http://www.nature.com/scientificreports).
3. Yin JZ, Yin HY, Chao YH & Shi HY. 2024d. Energy and tellurium deposits. *AIMS Geosciences*, 10 (1): 28-42. DOI: 10.3934/geosci.2024002.
4. Yin JZ, Xiang SP, Chao YH, Yin YH & Shi HY. 2023a. Petrochemical eigenvalues and diagrams for the identification of metamorphic rocks' protolith, taking the host rocks of Dashuigou tellurium deposit in China as an example. *Acta Geochimica*, 42 (1): 103-124. DOI: 10.1007/s11631-022-00583-6.
5. Yin JZ, Xiang SP, Yin HY, Shi HY & Chao YH. 2023c. Origin of the Dashuigou independent tellurium deposit at the southeastern margin of Qinghai-Tibet plateau: based on the abundances of trace elements in the country rocks. *Advances in Geological and Geotechnical Engineering Research*, 5 (4): 41-55. DOI: <https://doi.org/10.30564/agger.v5i4.5967>.
6. Yin JZ, Yin HY, Chao YH, Xiang SP & Shi HY. 2024a. Geology and geochemistry of the only independent tellurium deposit in the world. *Naturalis Scientias*, 1 (1): 1-31. DOI: <https://doi.org/10.62252/NSS.2024.1001>.
7. Yin JZ, Chao YH, Yin HY, Shi HY & Xiang SP. 2024c. Origin of the Dashuigou independent tellurium deposit at Qinghai-Xizang Plateau: constraints from the light stable isotopes C, O, and H. *Acta Geochimica*, DOI: 10.1007/s11631-023-00665-z. <https://doi.org/10.1007/s11631-023-00665-z>.
8. Murakami H & Ishihara S. 2013. Trace elements of indium-bearing sphalerite from tin-polymetallic deposits in Bolivia, China and Japan: A femto-second LA-ICPMS study. *Ore Geology Reviews*, 53: 223-243. DOI: 10.1016/j.oregeorev.2013.01.010.
9. Xu J & Li XF. 2018. Spatial and temporal distributions, metallogenic backgrounds and processes of indium deposits. *Acta Petrologica Sinica*, 34 (12): 3611-3626 (in Chinese with English abstract)
10. Mejías O, Parbhakar-Fox A, Jackson L, Valenta R & Townley B. 2023. Indium in ore deposits and mine waste environments: Geochemistry, mineralogy, and opportunities for recovery. *Journal of Geochemical Exploration*, 255. <https://doi.org/10.1016/j.gexplo.2023.107312>.
11. Hund K, La PD, Fabregas TP, Laing T & Drexhage J. 2023. Minerals for climate action: The mineral intensity of the clean energy transition.
12. Werner TT, Mudd, MG & Jowitt MS. 2017. The world's by-product and critical metal resources part III: A global assessment of indium. *Ore Geology Reviews*, 86: 939-956. DOI: <https://doi.org/10.1016/j.oregeorev.2017.01.015>.



13. Benites D, Torró L, Vallance J, Laurent O, Valverde PE, Kouzmanov K, Chelle-Michou C & Fontboté L. 2021. Distribution of indium, germanium, gallium and other minor and trace elements in polymetallic ores from a porphyry system: The Morococha district, Peru. *Ore Geology Reviews*, 136, 104236.
14. Andersen JC, Stickland RJ, Rollinson GK & Shail RK. 2016. Indium mineralisation in SW England: host parageneses and mineralogical relations. *Ore Geology Reviews*, 78, 213-238. DOI: 10.1016/J.OREGEOREV.2016.02.019.
15. Andersson P. 2020. Chinese assessments of “critical” and “strategic” raw materials: Concepts, categories, policies, and implications [J]. *The Extractive Industries and Society*, 7 (1): 127-137.
16. Schwarz-Schampera U & Herzig PM. 2013. *Indium: Geology, Mineralogy, and Economics* [M]. Springer Science & Business Media. DOI: 10.1007/978-3-662-05076-7.
17. Xu J, Cook NJ, Ciobanu CL, Li X, Kontonikas-Charos A, Gilbert S & Lv Y. 2021. Indium distribution in sphalerite from sulfide–oxide–silicate skarn assemblages: a case study of the Dulong Zn–Sn–In deposit, Southwest China [J]. *Mineralium Deposita*, 2021, 56: 307-324. DOI: 10.1007/s00126-020-00972-y.
18. Ye L, Cook NJ, Ciobanu CL, Liu YP, Zhang Q, Liu TG, Gao W, Yang YL & Danyushevskiy L. 2011. Trace and minor elements in sphalerite from base metal deposits in South China: A LA-ICPMS study [J]. *Ore Geology Reviews*, 39 (4): 188-217. DOI: 10.1016/j.oregeorev.2011.03.001.
19. Zhao Z, Hou L, Ding J, Zhang Q & Wu S. 2018. A genetic link between Late Cretaceous granitic magmatism and Sn mineralization in the southwestern South China Block: A case study of the Dulong Sn-dominant polymetallic deposit [J]. *Ore Geology Reviews*, 93: 268-289.
20. Schwarz-Schampera U & Herzig PM. 2002. *Indium, Geology, Mineralogy, and Economics*. Berlin, Heidelberg: Springer Science Business Media.
21. Zheng Y, Guo CL, Wang DH, Zhao T & Wang Y. 2023. Spatiotemporal distribution, genetic types and mineralization mechanism of associated indium (cadmium gallium germanium) deposits in China: summary and prospect. *Acta Geologica Sinica*, 97 (11): 3569-3603 **(in Chinese with English abstract)**.
22. China Economic Research Institute. September 1, 2023. *2023 China Indium Industry Market Research Report*. [https://www.sohu.com/a/716820994\\_120928700](https://www.sohu.com/a/716820994_120928700). Retrieved June 1, 2024 **(in Chinese)**.
23. Peng ZW. February 13, 2023. [https://www.sohu.com/a/438371240\\_120113054](https://www.sohu.com/a/438371240_120113054). Retrieved June 7, 2024 **(in Chinese)**.
24. Cook NJ, Sundblad K, Valkama M, Nygård R, Ciobanu CL & Danyushevsky L. 2011. Indium mineralisation in A-type granites in southeastern Finland: Insights into mineralogy and partitioning between coexisting minerals. *Chemical Geology*, 284 (1-2): 62-73. DOI:10.1016/j.chemgeo.2011.02.006.
25. Tu GC, Gao ZM, Hu RZ, Zhang Q, Wen HJ, Liu JJ, Zhang Z, Zhao ZH, Li CY, Cao ZM, Zhang BG, Lu JL, Liu TG, Yao LB, Qi HW, Zhuang HP, Ye L, Liu YP, Deng HL, Su WC & Zhang PH. 2004. *Dispersed element geochemistry and mineralization mechanism*. Beijing: Geological Publishing House. pp.424 **(in Chinese with English abstract)**.
26. Zhang Q, Zhu XQ, He YL, Jiang JJ & Wang DP. 2006. Indium enrichment in the Meng'en Tolgoi Ag-Pb-Zn deposit, Inner Mongolia, China. *Resource Geology*, 56 (3): 337-346. DOI:10.1111/rge.2006.56.issue-3 **(in Chinese with English abstract)**.
27. Ishihara S, Qin KZ & Wang YW. 2008. Resource evaluation of indium in the Dajing tin-polymetallic deposits, Inner Mongolia, China. *Resource Geology*, 58 (1): 72-79. DOI:10.1111/rge.2008.58.issue-1.
28. Zhang Q, Liu ZH, Zhan XZ & Shao SX. 2003. Specialization of ore deposit types and minerals for enrichment of indium. *Mineral Deposits*, 22 (1): 309-316 **(in Chinese with English abstract)**.
29. Cheng YS. 2013. Discussion on the distribution characteristics and production rules of indium-rich deposits [J]. *Acta Mineralogica Sinica*, (S2): 2. DOI: CNKI:SUN:KWXB.0.2013-S2-111 **(in Chinese with English abstract)**.
30. Liu JJ, Liu JM, Zheng MH, Zhou YF, Gu XX, Lin Y & Zhang B. 1998. Indium enrichment in Cambrian gold deposits in western Qinling and its significance. *Gold Science and Technology*, 6 (1): 24-25 **(in Chinese with English abstract)**.
31. Guo CL, Wang DH, Fu XF, Zhao ZG, Fu DM & Chen YC. 2006. Discovery of indium-rich ore in the Chahe tin mining area, Sichuan and its prospecting significance [J]. *Geological Review*, 52 (4): 550-555. DOI: 10.3321/j.issn:0371-5736.2006.04.014 **(in Chinese with English abstract)**.
32. Zhao YY, Liu Y, Cui YB, Lü LN, Song L & Qu XM. 2010. Discovery and significance of indium mineralization belt in Bangong Lake-Nujiang metallogenic belt and adjacent areas in Tibet [J]. *Geological Review*, 56 (4): 568-578 **(in Chinese with English abstract)**.



33. Wang SH, He S & Huang HX. 2014. Discovery of sulfide-indium copper ore in the Zijinshan copper-gold deposit in Fujian and its significance for deep prospecting [J]. *Geological Bulletin*, (9): 1425-1429. DOI: 010.3969/j.issn.1671-2552.2014.09.018 (in Chinese with English abstract).
34. Liu JP, Gu XP, Shao YJ, Feng YZ & Lai JQ. 2016. Indium mineralization in copper-tin stratiform skarn ores at the Saishitang-Rilonggou ore field, Qinghai, Northwest China. *Resource Geology*, 66 (4): 351-367. DOI: 10.1111/rge.2016.66.issue-4 (in Chinese with English abstract).
35. Liu JP. 2017. Indium mineralization in a Sn-poor skarn deposit: A case study of the Qibaoshan deposit, South China. *Minerals*, 7 (5): 76. DOI: 10.3390/min7050076.
36. Liu JP, Rong YN, Zhang SG, Liu ZF & Chen WK. 2017. Indium mineralization in the Xianghualing Sn-Polymetallic Orefield in southern Hunan, southern China. *Minerals*, 7 (9): 173. DOI: 10.3390/min7090173
37. Liu JP, Rong YN, Gu XP, Shao YJ, Lai JQ and Chen WK. 2018. Indium mineralization in the Yejiwei Sn-polymetallic deposit of the Shizhuyuan orefield, southern Hunan, China. *Resource Geology*, 68 (1): 22-36. DOI: 10.1111/rge.2018.68.issue-1 (in Chinese with English abstract).
38. Chen C & Zhao TP. 2021. Mineralization of indium in magmatic-hydrothermal systems [J]. *Mineral Deposits*, 40 (2): 206-220. DOI:10.16111/j.0258-7106.2021.02.002 (in Chinese with English abstract).
39. The mineralogy of indium. <https://www.mindat.org/element/Indium>. Retrieved July 23, 2024.
40. Yang T, Yang Z, Luo AG, Ran JD, Lü X, & Zhang R. 2018. A brief analysis of the distribution characteristics and ore-controlling factors of the indium-rich ore bodies in the Dulong polymetallic deposit, Wenshan. *Low Carbon World*. DOI:10.3969/j.issn.2095-2066.2018.07.043 (in Chinese with English abstract).
41. Zhang SK, Su H & Tao ZH. 2013. Re-understanding of the ore-controlling factors and genesis of the Dulong tin-zinc polymetallic deposit [J]. *Acta Geoscientia Sinica*, (s1). DOI:10.3975/cagsb.2013.s1.17 (in Chinese with English abstract).
42. Zhou JP & Xu KQ. 1997. Discussion on the genesis of tin polymetallic deposits in southeastern Yunnan [J]. *Yunnan Geology*, 16 (4): 41. DOI: CNKI:SUN:YNZD.0.1997-04-000 (in Chinese with English abstract).
43. Smith IC, Carson BL & Hoffmeister F. 1978. *Trace Metals in the Environment, Volume 5: Indium*. Ann Arbor: Ann Arbor Science Publishers.
44. Jenner FE & O'Neill HSC. 2012. Analysis of 60 elements in 616 ocean floor basaltic glasses. *Geochemistry, Geophysics, Geosystems*, 13 (2): Q02005.
45. Kovalenker VA, Jeleň S & Sandomirskaya S. 1993. Minerals of the system Ag-Cu-Pb-Bi-S from the polymetallic veins of the Štiavnica-Hodruša ore field (Slovakia). *Geologica Carpathica*, 44 (6): 409-419.
46. Witt-Eickschen G, Palme H, O'Neill HSC & Allen CM. 2009. The geochemistry of the volatile trace elements As, Cd, Ga, In and Sn in the Earth's mantle: New evidence from in situ analyses of mantle xenoliths. *Geochimica et Cosmochimica Acta*, 73 (6): 1755-1778. DOI:10.1016/j.gca.2008.12.013.
47. Anders E & Grevesse N. 1989. Abundances of the elements: Meteoritic and solar. *Geochimica et Cosmochimica Acta*, 53 (1): 197-214. DOI:10.1016/0016-7037(89)90286-X.
48. Taylor SR & McLennan SM. 1985. *The Continental Crust: Its composition and Evolution*. Oxford: Blackwell.
49. Liu YJ. 1984. *Elemental Geochemistry*. Beijing: Science Press.
50. Ohta E. 1991. Polymetallic mineralization at the Toyoha mine, Hokkaido, Japan. *Mining Geology*, 41 (229): 279-295.
51. Shimizu M & Kato A. 1991. Roquesite-bearing tin ores from the Omodani, Akenobe, Fukoku, and Ikuno polymetallic vein-type deposits in the Inner Zone of southwestern Japan. *Canadian Mineralogist*, 29 (2): 207-215.
52. Imai N & Choi SG. 1984. The first Korean occurrence of roquesite. *Mineralogical Journal*, 12 (4): 162-172. DOI:10.2465/minerj.12.162.
53. Seifert T & Sandmann D. 2006. Mineralogy and geochemistry of indium-bearing polymetallic vein-type deposits: Implications for host minerals from the Freiberg district, eastern Erzgebirge, Germany. *Ore Geology Reviews*, 28 (1): 1-31.
54. Shimizu T & Morishita Y. 2012. Petrography, chemistry, and near-infrared microthermometry of indium-bearing sphalerite from the Toyoha polymetallic deposit, Japan. *Economic Geology*, 107 (4): 723-735. DOI:10.2113/econgeo.107.4.723.
55. Seward TM, Henderson CMB & Charnock JM. 2000. Indium (III) chloride complexing and solvation in hydrothermal solutions to 350°C, an EXAFS study. *Chemical Geology*, 167 (1-2): 117-127. DOI: 10.1016/S0009-2541(99)00204-1.



56. Zhu XQ, Zhang Q, He YL & Zhu ZH. 2006. Study on the relationship between indium and tin, lead and zinc in ore-forming fluids of indium-rich and indium-poor deposits. *Geochemistry*, 35 (1): 6-12. DOI:10.3321/j.issn:0379-1726.2006.01.002.
57. Zhang Q, Zhu XQ, He YL & Zhu ZH. 2007. In, Sn, Pb and Zn contents and their relationships in ore-forming fluids from some in-rich and in-poor deposits in China. *Acta Geologica Sinica*, 81 (3): 450-462. DOI:10.1111/acgs.2007.81.issue-3.
58. Chen LY, Zhang ZD & Wang WZ. 2008. Self-assembled porous 3D flowerlike  $\beta$ -In<sub>2</sub>S<sub>3</sub> structures: Synthesis, characterization, and optical properties. *The Journal of Physical Chemistry C*, 112 (11): 4117-4123. DOI:10.1021/jp710074h.
59. Datta A, Sinha G, Panda SK & Patra A. 2009. Growth, optical, and electrical properties of In<sub>2</sub>S<sub>3</sub> zigzag nanowires. *Crystal Growth and Design*, 9 (1): 427-431. DOI:10.1021/cg800663t.
60. Sugaki A, Ueno H, Shimada N, Kusaschi I, Kitakaze A, Hayashi K, Kojima S & Sanjines O. 1983. Geological study on the polymetallic ore deposits in the Potosi district, Bolivia. *Science Reports, Tohoku University (Series III)*, 15: 409-460.
61. Jovic SM, Guido DM, Melgarejo JC, Páez GN, Ruiz R & Schalamuk IB. 2011a. The indium-bearing minerals of the pingüino polymetallic vein system, Deseado Massif, Patagonia, Argentina. *The Canadian Mineralogist*, 49 (4): 931-946. DOI:10.3749/canmin.49.4.931.
62. Jovic SM, Guido DM, Ruiz R, Paez GN & Schalamuk IB. 2011b. Indium distribution and correlations in polymetallic veins from Pingüino deposit, Deseado Massif, Patagonia, Argentina. *Geochemistry: Exploration, Environment, Analysis*, 11 (2): 107-115. DOI:10.1144/1467-7873/09-IAGS-013.
63. Jovic SM, Guido DM, Schalamuk IB, Ríos FJ, Tassinari CCG & Recio C. 2011c. Pingüino in-bearing polymetallic vein deposit, Deseado Massif, Patagonia, Argentina: Characteristics of mineralization and ore-forming fluids. *Mineralium Deposita*, 46 (3): 257-271. DOI:10.1007/s00126-010-0324-5.
64. Valkama M, Sundblad K, Nygård R & Cook N. 2016a. Mineralogy and geochemistry of indium-bearing polymetallic veins in the Sarvialxviken area, Lovisa, Finland. *Ore Geology Reviews*, 75: 206-219. DOI:10.1016/j.oregeorev.2015.12.001.
65. Li XF, Yasushi W & Mao JW. 2007. Research situation and economic value of indium deposits. *Mineral Deposits*, 26 (4): 475-480 (in Chinese with English abstract).
66. Li XF, Yang F, Chen ZY, Bu GJ & Wang YT. 2010. A tentative discussion on geochemistry and genesis of indium in Dachang tin ore district, Guangxi. *Mineral Deposits*, 29 (5): 903-914 (in Chinese with English abstract).
67. Cantinolle P, Laforet C, Maurel C, Picot P & Grangeon J. 1985. Contribution à la minéralogie de l'indium: Découverte en France de deux nouveaux sulfures d'indium et de deux nouvelles occurrences de roquesite. *Bulletin de Minéralogie*, 108 (2): 245-248.
68. Moura MA, Botelho NF, Olivo GR, Kyser K & Pontes RM. 2014. Genesis of the Proterozoic Mangabeira tin-indium mineralization, Central Brazil: Evidence from geology, petrology, fluid inclusion and stable isotope data. *Ore Geology Reviews*, 60: 36-49. DOI:10.1016/j.oregeorev.2013.12.010.
69. Sinclair WD, Kooiman GJA, Martin DA and Kjarsgaard IM. 2006. Geology, geochemistry and mineralogy of indium resources at Mount Pleasant, New Brunswick, Canada. *Ore Geology Reviews*, 28(1): 123-145.
70. Wu FY, Liu XC, Ji WQ, Wang JM & Yang L. 2017. Identification and research of highly fractionated granites. *Science China (Earth Sciences)*, 47 (7): 745-765.

#### Data availability

The data that support the findings of this study is available from the author upon reasonable request.

#### Declaration of competing interest

The author declares that he has no known competing financial interests or personal relationships that could have appeared to influence the work reported in this paper.

#### Use of AI tools declaration

The author declares that he has not used Artificial Intelligence (AI) tools in the creation of this article.





## Book Review

**Joy and Sorrow; Sorrow and Joy**Sean Daly<sup>1</sup> **Abstract**

This book, my second published book is dedicated to my son, Frank Daly who died an untimely death in November of 2021 and the first two poems are about him. This is a book of poetry written over about 59 years of my life and also it includes popular sayings, many from a very wise Salvadoran grandmother who lived in the mining town of El Mochito in Honduras for many years. The poems are written about family, philosophical topics, and with musings principally about mining and surveying, mineral exploration and Latin America and it was published in January of 2024 and is about 16,000 words long. This book was published by Friesen Press as it was my first book *From the Erzgebirge to Potosi* about the history of geology and mining in the last 500 years and also the close connection between mining, geology and society especially of the Renaissance and the Industrial Revolution.

**Key words:** True Americans; Latin America; mining projects; popular sayings; dedication to my son; “talking” rocks

---

**Affiliation Info:** <sup>1</sup>Deciphearth, PH4 4838 Fraser St, Vancouver BC V5V 4H4, Canada

**Article Info:** Received: 8 June 2024 / Revised: 17 June 2024 / Accepted: 30 June 2024 / Published Online: 30 June 2024.  
www.naturalisscientias.com

**Authors' Contact Info:** Daly, S: dalyshone24@gmail.com

**Citation:** Daly, Sean. 2024. Joy and Sorrow; Sorrow and Joy. *Naturalis Scientias*, 1 (2): 181-185. DOI: <https://doi.org/10.62252/NSS.2024.1013>.

**Copyright** © 2024 by the author. Published by *Naturalis Scientias*. This is an open access article under the Creative Commons Attribution-NonCommercial 4.0 International (CC BY-NC 4.0) License. (<https://creativecommons.org/licenses/by-nc/4.0/>).

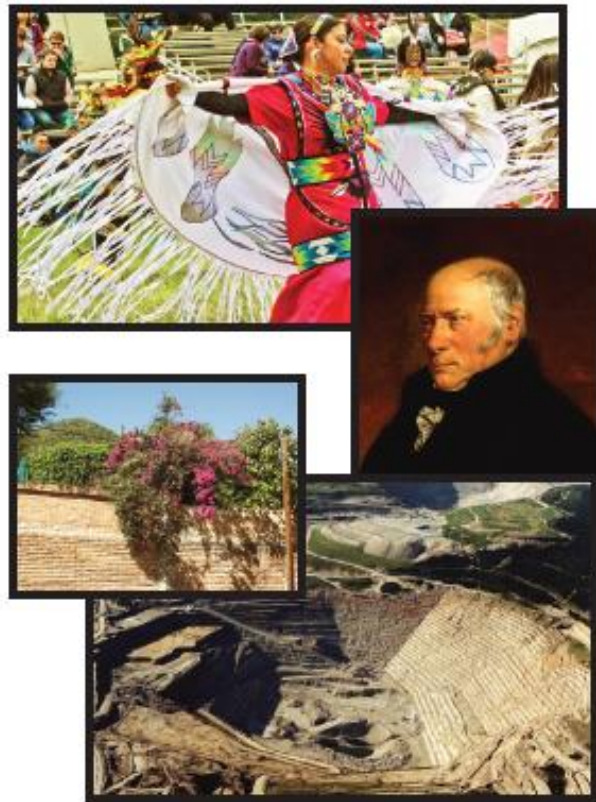
**Corresponding Author** : Sean Daly is a retired mining geologist with a BSc in geology and a MEng in mining engineering both from UBC and he worked 19 years at the large Highland Valley copper mine in south central British Columbia, Canada; Email: dalyshone24@gmail.com.



I am ‘switching gears’ as they used to say at the open pit mine where I worked for many years and have recently edited a short book of poems I have written over the years, for publishing (published in January of this year) The poems are about mining and surveying, family, Latin America and philosophy and life. These themes are all intertwined as I was a mining geologist but while working in Honduras got married to a beautiful woman both physically and in her heart and also have travelled extensively in both Canada and the US and also Latin America so hope my poems are imbued with what it is like to not just be a Canadian but also a true American in the sense of having lived and worked in various parts of the vast Americas from the Yukon and Alaska all the way to Punta Arenas in the Straits of Magellan.

# Joy & Sorrow

SORROW & JOY-MUSINGS ON MINING,  
FAMILY, LATIN AMERICA AND SOCIETY



Peter Sean Daly

Figure 1. The front cover of the book *Joy and Sorrow; Sorrow and Joy*

A relevant observation as to why I like writing is that geologists are much more into writing than engineers probably since they have to describe rocks and soils and their complex natural occurrences whereas engineers often deal with man-made materials like steel and plastic whose properties are known much more precisely and unequivocally. My latest and second book was published in January of this year and is called Joy and Sorrow; Sorrow and Joy because it deals in part with the two opposite emotions, both quite poignant, especially our grief for the untimely death of my son.

As true 'Americans' we are all conscious of the high mountain spine (the Western Cordillera) that occupies the western edge of North and South America, of having indigenous peoples asserting their rights in all of these countries, and of their artifacts and also ancient ruins of their temples and fortifications of places like Teotihuacan near Mexico City, of meeting mixed or mestizo or metis people in most of these countries where the people are a rich mixture of white ex-English, Scottish, Irish and Spanish and a few other Caucasian groups origin and of course indigenous and also from afro-descendent people. Also, we have common foodstuffs like corn and beans throughout these countries and various forms of tortillas, like the pupusas of El Salvador, the large and small tortillas of respectively Mexico and Central America and the very thick arepas of Venezuela, the rich mineral resources throughout these countries and the common brotherhood of the miners who face similar conditions from Alaska and the Yukon to the US and Mesoamerica and South America in dealing with corporations who usually are only out for the profit motive with a few exceptions.



**Figure 2.** The large Highland Valley Copper open pit Valley Copper in the foreground and the Lornex pit in the background

This poetry pamphlet also includes some very wise popular sayings heard from my experiences in the Americas and especially from a wise old grandmother from El Salvador on life from the perspective of those engaged in their local mining industry but of wide philosophical import, i.e. with universal truths. My website is: [www.seandalyauthor.com](http://www.seandalyauthor.com), for reading about my books content and ordering While this book.

While this book is partly about family and philosophical issues it also has a major section on mining and geotechnical work vicissitudes i.e. on the valiant struggle for production and scientific experiment experienced every day by the various types of mine workers be they miners, pipe fitters, electricians, geologists and engineers to name some of them. And lastly but not least, is the fact that the rocks 'talk' to you and you need to learn to listen to

them or else an accident could occur. Two examples were at the Bonanza Ledge gold small open pit mine near Wells, BC, Canada. The first was when I found a different rock type not the normal pervasive metamorphic phyllite (similar to a slate) and was reticent about really coming to grips with it on the first bench in it. But on the second bench on the same unit I had to listen to it as it was asserting itself by repetition so then I recognized it as actually a quartzite not a phyllite at all. Secondly, every time we mined within or just below the major fault/vein in one wall of the same pit it would slough. So on the third time we had mined about two benches below it and the snow was thawing and the fault was sloughing constantly. At that moment, or well before I should have put two and two together and warned of an imminent collapse. The fault material was just too weak and soil-like to hold up, due to a hydrothermal alteration halo that enveloped the fault and also intense fracturing. So sure enough it sloughed significantly and fortunately it happened right at shift change so no one was hurt. So it is not enough to make observations but conclusions need to be drawn quickly about how it will affect the operation and the personnel especially when it repeats its message saying “pay attention”. There is always warning in any instability. Also within and below this fault it was being double benched so steepening the slope where it couldn’t stand to be steepened. So the lesson is, as a geologist or geotechnical person it is of utmost importance to “listen to the rocks” and be open to what they tell you. And probably the most profound saying of my wife’s grandmother is “hay que saber vivir” or “you have to know how to live” which means at the same time as say working for a large mining corporation, whose main goal is profit so that one has to work hard to help them make this profit, if one is open about one’s environmentalism, say, then one can get chosen to help with mine waste dump reclamation and not give up one’s principles.



**Figure 3.** The underground very rich El Mochito Mine in Honduras with silver lead, zinc and cadmium

#### **Data availability**

The data that support the findings of this study is available from the author upon reasonable request.



**Declaration of competing interest**

The author declares that he has no known competing financial interests or personal relationships that could have appeared to influence the work reported in this paper.

**Use of AI tools declaration**

The author declares that he has not used Artificial Intelligence (AI) tools in the creation of this article.





## Book Review

**My impressions after reading the book *Less Words but Earnestly Practice--My Father Chuangan Zhang***JZ Yin<sup>1,2,3</sup> **Abstract**

Earlier in 2019, a non-fiction biography titled *Less Words but Earnestly Practice-My Father Chuangan Zhang* was published in Beijing, China. The subject of the biography is Professor Chuangan Zhang, an old-generation petroleum geologist in China. The author is Professor Zhang's youngest daughter, Mrs. Erping Zhang, a scholar who studies the history of Chinese geological sciences but has now retired. The book uses refined language to tell the story of Professor Zhang's life, especially his experience of studying and looking for oil in the northwest during the turbulent World War II. It also tells the fate of intellectuals before and after the change of power in China, as well as the patriotism and ambitions, personal ups and downs, and various opportunities and hardships of Chinese intellectuals in the great era.

**Key words:** Rare metal indium; primary associated deposit; genetic type; global temporal and spatial distribution; genesis

---

**Affiliation Info:** <sup>1</sup> College of Earth Sciences, Jilin University, Changchun 130061, China; <sup>2</sup> Wuhan Institute of Technology, Wuhan 430205, China; <sup>3</sup> Orient Resources Ltd., Canada

**Article Info:** Received: 15 May, 2024 / Revised: 30 May 2024 / Accepted: 7 June 2024 / Published Online: 30 June 2024.  
www.naturalisscientias.com

**Authors' Contact Info:** Yin, JZ: jzyin7@jlu.edu.cn

**Citation:** Yin, JZ. 2024. My impressions after reading the book *Less Words but Earnestly Practice--My Father Chuangan Zhang*. *Naturalis Scientias*, 1 (2): 186-196. DOI: <https://doi.org/10.62252/NSS.2024.1014>.

**Copyright** © 2024 by the authors. Published by *Naturalis Scientias*. This is an open access article under the Creative Commons Attribution-NonCommercial 4.0 International (CC BY-NC 4.0) License. (<https://creativecommons.org/licenses/by-nc/4.0/>).

**Corresponding Author** : Yin, JZ, PhD, PGeo, Professor; Email: jzyin7@jlu.edu.cn

## 1

I recently finished reading the book titled *Less Words but Earnestly Practice--My Father Chuangan Zhang* (Figure 1, hereafter referred to as *Less Words but Earnestly Practice*) written by Erping Zhang for her father, Professor Chuangan Zhang, a previous generation Chinese petroleum geologist.



**Figure 1.** The front cover of the book *Less Words but Earnestly Practice*

As I read through the book without being able to put it down, I was greatly moved by the rusticity, simplicity, and purity of traditional Chinese intellectuals of that era, especially their great patriotic feelings for the country and the nation (Figure 2).



**Figure 2.** On April 27, 1947, Chuangan Zhang (right) was working in the field in Kongtong Mountain, Pingliang, Gansu, China

At the same time, I am also saddened at the thought of not being alive during one of China's golden periods as described in the book

At the same time, I am also saddened at the thought of not being alive during one of China's golden periods as described in the book.

The reason why the Republic of China is said to be one of the few “Golden Ages” in Chinese history is because Chinese intellectuals at the time could devote themselves to modern scientific research without worry for politics, severe criticism, prison, or potentially death. Despite the poor material and economic conditions, Chinese geologists were able to make the best of what they had (Figures 3 and 4). Field geological surveys could only rely on camels, donkeys, horses and ox carts for transportation, and more often than not, on manual labor. Comparatively speaking, geologists in western developed countries had already driven cars to conduct field geological surveys and research.



**Figure 3.** In May 1947 Chuangan Zhang took a photo during the petroleum geological survey in the Liuhu area of Pingliang, Gansu, China



**Figure 4.** On May 7, 1946, Sun, C.C., (first from left), director of the Geology Division of the Gansu Petroleum Mining Bureau, and Zhang Chuangan (second from left), were in the camp when they were conducting petroleum geological surveys in the western basin of Jiuquan, Gansu, China

Despite these hardships, the book shines in its portrayal of the strong friendships and bonds between people at that time, and creates a vivid and touching story for the reader (Figures 5 and 6).



**Figure 5.** On January 5, 1946, the staff of the Geology Division of Yumen Oil Mine in Gansu of China took a group photo at the No. 50 oil well. The one on the left sitting on the tire is Chuangan Zhang, the middle is Sun, C.C.



**Figure 6.** On April 9, 1948, Chuangan Zhang (right) and Tian Zaiyi (left) were in Yantan, Pingliang, Gansu, China

The author conveys the understanding that these friendships do not just last for a moment, but carry on for the lifetimes of these individuals (Figure 7).



**Figure 7.** On January 10, 2009, Zhang Chuangan (middle in the front row) took a group photo in Beijing on his 90th birthday

If pioneers such as Xie Jiarong (Hsieh, C.Y., 1897-1966) and Sun Jianchu (Sun, C.C., 1897-1952), who started petroleum geology research in the 1920s and 1930s, were the first generation of petroleum geologists in China, then in the 1940s, Zhang Chuangan and other people who joined the ranks can be regarded as the second generation of Chinese petroleum geologists. Even in the turbulent and chaotic backdrop of World War II, these two generations of petroleum geologists who were fighting on the front lines still discovered many "oil seedlings", resulting in great breakthroughs in oil discovery and development in China after 1949 (Figure 8).



**Figure 8.** Taken in Yumen, Gansu, China around October 1945. From left: Weng Wenbo, Li Desheng, Zhang Chuangan, Bian Meinian, and Tian Zaiyi

The so-called "Golden Age" in this article refers to the Republic of China period before 1949. The term "Golden Age" is not my own invention, but the common view of many senior Chinese intellectuals and much of the modern scientific community. Notably, several Chinese artists once made a film about the literati of that period, similarly titled "Golden Age". One of the protagonists of the film is Xiao Hong, a great female writer who both was born and died at a young age during the Republic of China.

## 2

After the tides turned in 1949, these petroleum geologists and contemporary intellectuals experienced fear and torture as a result of various political movements, and experienced countless hardships such as hunger and extreme mental distress. Some even needlessly took their own lives. For example, Xie Jiarong, one of the important founders of China's geological undertakings, and his wife both committed suicide. The book also describes Mr. Zhang's college classmate Mr. Wang Jianzhi, chief geologist of Yumen Petroleum Administration Bureau, who was hanged and beaten to death during the Cultural Revolution of China in 1960s.

Nevertheless, the Chinese intellectuals represented by Mr. Zhang still have no complaints and no regrets. They continue to uphold the spirit of selfless dedication of Chinese traditional intellectuals to the nation and the country, and have continued their diligent pursuit of minerals on this ancient land (Figure 9).



**Figure 9.** On June 7, 1982, Chuangan Zhang (sitting in the front row) and others carried out a field geological survey in the Tianshan Mountains, Xinjiang, China

## 3

Chuangan Zhang (1920-2014), was born to a peasant family in Tai'an, an ancient city at the foot of Mount Tai in Shandong Province, China. He attended a rural private school that was very common in China at that time to learn to read and write. In 1928, he transferred to a new primary school and began a traditional Chinese education. In 1937, he was admitted to Shandong Jinan High School. On November 14 of the same year, because of the Japanese invasion of China, he moved westward with more than 100,000 students in exile. During this period, he was admitted to the Jining Military Academy. In 1938, it was incorporated into the National Hubei Middle School. The school has been renamed several times: first it was renamed National Mianyang Middle School, and then it was changed to National Sixth Middle School. This was also quite in line with the ever-changing world at that time (Figure 10).



Figure 10. Zhang Chuangan when he graduated from middle school in 1937

In 1941, Mr. Zhang was admitted to the Geology Department of Central University (Figure 11), which moved west to Chongqing at that time, and joined the Geological Society of China in 1944 during his studies.



Figure 11. Photo of Zhang Chuangan when he was admitted to China National Central University in 1941

After graduating in 1945, Mr. Zhang worked in the Geology Division of Yumen Oil Mine in Gansu Province, the first oil field in China. Since then, he has become associated with petroleum geology and has been engaged in various oil and gas explorations throughout Northwest China, including Lanzhou in Gansu, Nanjing in Jiangsu, Beijing, Tianjin, Xi'an in Shaanxi, and Yinchuan in Ningxia. During this period, Mr. Zhang successively followed Mr. Xie Jiarong, the pioneer of Chinese geology, and Mr. Sun Jianchu, the pioneer of China's petroleum geology, to engage in petroleum geological exploration (Figure 12).



**Figure 12.** In the spring of 1945, Zhang Chuangan (first from the right) and his colleagues took pictures during the interval of field geological survey in Kongtong Mountain, Pingliang, Gansu, China

In April 1949, Mr. Zhang married Ms. Qi Wu in Lanzhou, and they had three daughters after marriage. The second daughter among them is Ms. Erping Zhang, the author of this book (Figure 1).

After the "Cultural Revolution of China" ended in the autumn of 1979, Mr. Zhang's family officially settled in Beijing, and he himself continued to engage in petroleum geology research and trained five graduate students, two of whom later became academicians of the Chinese Academy of Engineering (Figures 13, 14, and 15).



**Figure 13.** In July 1983, Chuangan Zhang investigated petroleum geology in the Yousha (oil sand) mountain of the Qaidam Basin in Qinghai, China



**Figure 14.** Around 1964, Zhang Chuangan (right) and his colleague Zhao Qiming



**Figure 15.** On January 31, 1996, Zhang Chuangan (second from left) took a group photo with his classmates in Beijing



**Figure 16.** On December 27, 1995 in Beijing, a group photo was held to celebrate the 50th anniversary of Professor Zhang Chuangan (second from left) engaged in petroleum geology

Mr. Zhang spent most of his life engaged in petroleum geological exploration in the Ordos Basin in Northwest China, namely the famous Changqing Oilfield and Tarim Basin after 1970. While he and his colleagues found areas with oil potential, they also accidentally explored the Jurassic coalfields on the Ordos Platform. The coalfield made a major breakthrough in the 1980s. Among them, the Shenfu-Dongsheng coalfield has reserves of 230 billion tons, ranking first among the eight largest coalfields in the world at the time and the largest coalfield in China.

Mr. Zhang is a free-thinking person, with an optimistic and humorous nature. As a result, he has excellent popularity among his peers and is widely respected by the broader community.

#### 4

The book *Less Words but Earnestly Practice* was published by Geological Publishing House in Beijing in early 2019. In addition to the concise preface, postscript and name index, the whole book is mainly composed of the following five chapters:

- **Chapter 1:** Family background and school experience
- **Chapter 2:** Entering Ordos for the first time
- **Chapter 3:** From Nanjing to Xi'an
- **Chapter 4:** Twenty-one years in Yinchuan
- **Chapter 5:** Returning and Settling in Beijing

The book has 190 pages and 200,000 Chinese characters.

It is worth mentioning that although this book is the biography of the author with her father as the theme, it deeply reflects the social outlook, political ecology, and sophistication of people in China from the 1920s through the turn of the millennium. The author of the book is an expert in the study of the history of geology in China, and has acquired countless first-hand materials through decades of her professional accumulation. However, in order to



complete the book with greater precision and make it stand the test of time, she specifically visited countless old relatives, friends, and colleagues of her father during his lifetime. In this sense, the book is not just a biography about Mr. Zhang himself, but a rare historical material of the initiation and development of petroleum geology in China.

The text is vivid and beautiful, and conveys the sense of chatting with relatives and friends, resulting in a book that is easy to read.

As mentioned at the beginning of this article, the author of this book, Zhang Erping, a senior engineer in geological history in China, is the second daughter of Mr. Zhang Chuangan.

Since 1972, she has successively engaged in field geological work, geological mapping and research on the history of geology of China. She has published more than 60 research articles on the history of Chinese geological institutions and geologists in various newspapers and magazines. After retiring, she served as the executive editor-in-chief of books such as "History of China Geological Library" and "History of China's Geological Survey in One Hundred Years". She is currently a member of the Geological History Committee of the International Union of Geological Sciences, and a vice-chairman of the Geological History Committee of the Geological Society of China.

All the pictures in this article are provided by the author of the book, Ms. Erping Zhang.

**Data availability**

The data that support the findings of this study is available from the author upon reasonable request.

**Declaration of competing interest**

The author declares that he has no known competing financial interests or personal relationships that could have appeared to influence the work reported in this paper.

**Use of AI tools declaration**

The author declares that he has not used Artificial Intelligence (AI) tools in the creation of this article.

